PEM Fuel Cell Water And Thermal Management: A Methodology to Understand Water and Thermal Management in an Automotive Fuel Cell System

BY

PARAVASTU BADRINARAYANAN
B.E. (Birla Institute of Technology and Science, Pilani, India) 1999

THESIS

Submitted in partial satisfaction of the requirements for the degree of

MASTER OF SCIENCE

In

Transportation Technology & Policy

in the

OFFICE OF GRADUATE STUDIES

of the

UNIVERSITY OF CALIFORNIA

DAVIS

Approved:

_____(Chair)

_____

_____

Committee in Charge

2001

To
Amma and Appa

Acknowledgments

It is one of life's simple pleasures to say thank you for all the help that one has received. I would like to thank the staff and the researchers of the Fuel Cell Vehicle Modeling Program, UC Davis without whose help this project would not have taken place. Specifically, I am grateful to Dr. Robert Moore, Director, Fuel Cell Vehicle Modeling Program for his confidence in me. I feel that I have learnt a lot under his guidance. I would like to thank Prof. Myron Hoffman for his patience and guidance during the course of this project. I would like to specially thank Dr. Sitaram Ramaswamy for his encouragement and constant reassurance that I was on the right track. Special thanks also goes to Anthony Eggert, colleague and friend, for his valuable insight and discussions in water and thermal management modeling. I am thankful to the other members of the Fuel Cell Vehicle Modeling Program- Joshua Cunningham, Karl Hauer, Meena Sundaresan, David Friedman, Fernando Contadini, Monterey Gardiner, Claudia Diniz and Peter Vagadori. Thank you all.

Abstract

This report presents a methodology to study fuel cell system water and thermal management. The primary objective is to illustrate a methodology that will help a fuel cell system design engineer in understanding the impacts of various parameters on the water and thermal management of the fuel cell system and to aid in devising optimal control strategies. This study has been driven by the dearth of public literature on water and thermal management in automotive fuel cell systems.

First, the requirement of "tools" (models) for such a study is presented. Stack, radiator and condenser models are developed according to the requirements. The tools that are developed are then used for a specific case of a load following direct hydrogen fuel cell vehicle. In the analysis that ensues, the impact of various parameters such as pressure, flow rates and humidification temperatures on the stack are performed. It is made clear that understanding the water transport processes inside a fuel cell is an essential step before devising optimal control strategies for the fuel cell system.

On the anode side, the impact of the anode saturation temperature is studied at the stack and system level. It is shown that though there might be a benefit in stack performance by increasing the anode saturation temperature above the cell operating temperature, there may not be any gain in system performance.

On the cathode side, the impact of pressure and stoichiometry on water and thermal management is studied. As a result, the trade-off between water recovery at the

stack and the condenser is explained. Finally, the implication of the water and thermal management parameters on devising optimal control strategies is discussed.

Table of Contents:

List of Illustrations:

1. Introduction

1.1 Water and Thermal Management in Fuel Cell Systems: A Background

Proton exchange membrane (PEM) fuel cell systems are being considered as potential substitutes for internal combustion engines in automobiles (Panik 1998, Kalhammer 1998). The primary driver in the short term for fuel cell vehicles (FCV) in the United States has been the need to mitigate the worsening air quality conditions in the major cities. FCVs are expected to play a major role as an alternative in meeting the California's zero emission vehicle (ZEV) mandate (Kenny 1998) that requires 10 % of the vehicles sold by the automotive manufacturers after year 2004 to be ZEVs (CARB 2000). Also, FCVs offer the potential of high efficiency (Panik 1998) and reduced carbon dioxide emissions thereby making them potential candidates for European auto companies to meet their voluntary carbon dioxide emission limits in the European Union (Bauen and Hart 2000).

There are several technical issues that have to be resolved before fuel cell systems can become a commercial reality for automotive applications. One of the technical issues in fuel cell system development is water and thermal management (WTM). Proper WTM is essential for maximizing the performance of a fuel cell system (Fronk 2000, Eggert 2000).

All the analysis in this report will focus on *PEM* fuel cell systems, as they are the class of fuel cell systems currently considered by automakers. (Kalhammer 1998, Panik 1998)

Specifically, some of the WTM issues are as follows:

1. Currently considered PEM electrolyte in the fuel cell needs to be hydrated at all times of operation to prevent high ionic resistance that can potentially lead to failure of the membrane (Prater 1994). Maintaining water balance in the cells requires maintaining optimal conditions (pressure, stoichiometry and humidity) in the anode and cathode side. Determining these optimal conditions necessitates understanding the physical processes that occur inside the fuel cell. As will be discussed in this chapter, several studies have attempted at understanding the interactions, but all the interactions still remain to be unearthed.
2. Fuel cells, just like any other energy conversion device, are not 100% efficient. The amount of fuel energy that cannot be converted to useful electrical energy has to be rejected as heat. Current fuel cells operate at temperatures between 70 and 90 C (Prater 1994) as opposed to temperatures of 200 - 400 C (cylinder combustion surface temperature) in internal combustion engines (Heywood 1988). Also, all the waste heat in the fuel cell system has to be removed by the radiator as opposed to the internal combustion engine where some of the heat is taken away by the exhaust (Sadler et al. 2001). Hence, heat rejection to the ambient becomes difficult compared to conventional internal combustion engine

due to a lower temperature driver (Fronk et al. 2000). The "difficulty" either means large heat exchange equipment or large parasitic loads such as radiator fan power.

3. The fuel cell system requires water for several processes such as humidification of the streams and for fuel processing (in the case of indirect-hydrocarbon fuel cell systems). For easy consumer operation of fuel cell vehicles, it would be beneficial to achieve "water balance" in a fuel cell system. In other words, the water needed by the system would be recovered in the system itself (as the fuel cell produces water that can potentially be recovered). This requirement plays into dictating the operating conditions such as pressure and flow rates (Friedman et al. 2001, Badrinarayanan[2] et al. 2001). Also, this requirement potentially increases the parasitic loads of the WTM system.

The next section will highlight the thesis of this study and will detail the structure of this report.

1.2 Thesis and Report Structure

The heart of any thesis lies in the questions it attempts to answer. This section discusses the two broad questions that have been addressed in this thesis.

1. The first question, a general one, is how does one go about analyzing the water and thermal management requirements of an automotive fuel cell system. What are the tools one would require to do such an analysis?
2. In a fuel cell system, there are many operating parameters such as pressure, flow rate, temperature and humidity of the anode and cathode streams, current density of the stack and so on. It is imperative to understand the complex interactions of varying these parameters, especially the ones that impact more than one component, before one can begin to devise optimal operating strategies. Three parameters have been identified and the impact of their variation has been studied in the context of water and thermal management. The parameters are the anode saturation temperature, the cathode pressure and cathode flow rate. How do these parameters affect the performance of the fuel cell system?

Report Structure: The next section in this chapter will give a brief account of fuel cell and fuel cell system operation. The final section in this chapter lists all the major studies that have been done in the area of PEM fuel cell water and thermal management. The second chapter focuses on the modeling methodology employed in this analysis. The details of the various models of the components used in this study will be outlined here. The third chapter titled, "Anode-Centric Analysis", attempts at studying the impact of varying the anode saturation temperature at the stack and the system level. The fourth chapter titled, "Cathode-Centric analysis", examines the effect of varying the cathode pressure and flow rate from a water and thermal management perspective. Implications of water and thermal management parameters on devising optimal operating strategies for

the cathode will be investigated here. *It should be borne in mind that the anode-centric and cathode-centric analysis are independent studies. The models and configurations of the components are different. The reader should refrain from making any quantitative comparisons between them. The reasons for this will be explained in the second chapter.*

1.3 Fuel Cell Fundamentals

This section gives an overview about fuel cells and fuel cell systems. Readers who are fairly acquainted with PEM fuel cell system fundamentals can comfortably skip this section.

Fuel Cell System

This section provides an overview of the processes that occur inside a direct-hydrogen fuel cell system. The system configuration described in this section is just a simple example of how a system can be designed.

Figure 1 shows a general schematic of a direct-hydrogen fuel cell system. The fuel supply system, possibly a hydrogen storage tank, supplies hydrogen to anode side of the fuel cell stack. This stream is humidified and conditioned prior to its entry into the stack. An air supply system (a compressor or a blower) supplies ambient air to the cathode side of the stack. This stream is conditioned prior to its entry into the cathode. A coolant loop is used to remove the heat generated due to inefficiency of the stack, as the

stack need to be maintained at 70 –90 C for optimal operation. The radiator attempts to maintain the stack coolant at around 80 C. A condenser is placed at the cathode exhaust to aid in water recovery. The system is designed to operate in water neutrality i.e. the water required for the system at any instant for the process of humidification of the streams is recovered in the system itself. The air-supply system, the coolant pump (shown by "P" in the radiator loop), the radiator fan and the condenser fan run off the electric power generated by the stack. The purpose of this section is to give the reader an idea of the system that will be dealt with in this thesis. The details regarding humidification, stack cooling and water recovery will be dealt with in detail later.

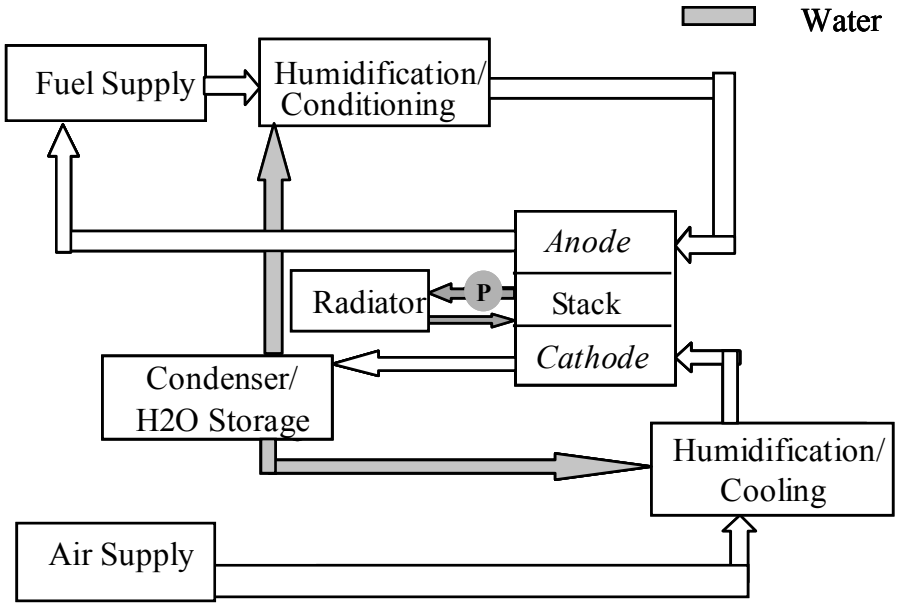

Figure 1: Schematic of a Direct –Hydrogen Fuel Cell System

The Fuel Cell

Simply defined, a fuel cell is an electrochemical device that converts the chemical energy of a fuel directly into electricity. An illustration of how a PEM fuel cell works is shown in Figure 2.

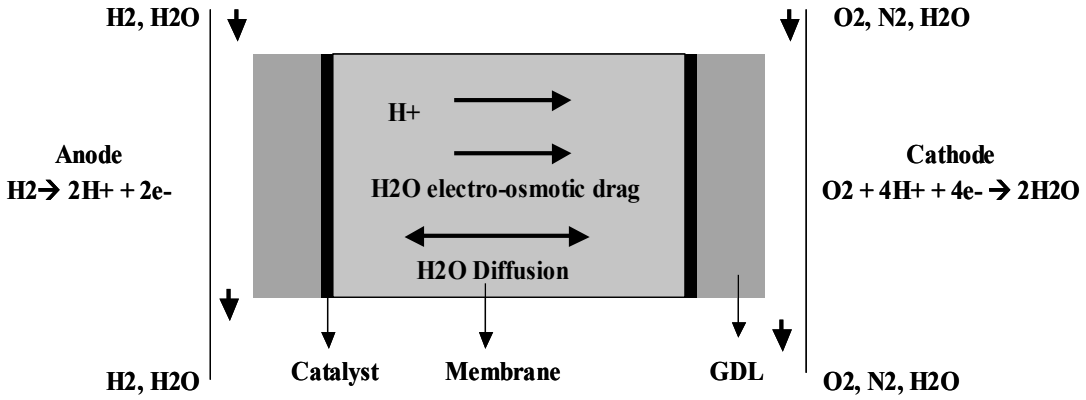

Figure 2: A Schematic of a hydrogen-oxygen fuel cell

A PEM fuel cell has a polymer as its electrolyte. This polymer is usually a good protonic conductor but a poor electronic conductor. Commercially available sources of these polymers are DuPont (makers of Nafion®), Dow, Asahi Glass (Japan), Asahi Chemicals (Japan) and W.L. Gore (Gottesfeld and Zawodzinski 1997). The catalyst layer, typically made up of a noble metal such as platinum supported on carbon, is deposited onto the membrane (Gottesfeld and Zawodzinski 1997). A gas diffusion-backing layer that helps in uniform distribution of the reactants is usually a carbon cloth that is pressed against the catalyst layer. The assembly of the gas diffusion layers, the

catalyst layers and the membrane is called the membrane-electrode assembly or the MEA[1]. Many such cells connected in series constitute a fuel cell stack.

When a humidified hydrogen stream is passed through the anode channel, hydrogen diffuses across the gas diffusion backing layer (GDL), and at the anode catalyst sites dissociate into protons and electrons as shown by the equation on the anode side in Figure 2. The protons get transported across the membrane and react with oxygen ions generated at the cathode catalyst layer. The electrons take the external circuit (not shown in figure) and reach the cathode side to aid in the formation of oxygen ions. Oxygen, similar to hydrogen on the anode side, has to diffuse through the gas diffusion layer to reach the cathode catalyst sites.

When the protons travel across the membrane from the anode to the cathode side, they tend to drag some water molecules with them. This phenomenon is known as *electro-osmotic drag*. Electro-osmotic drag is usually represented by the ratio of moles of water dragged per mole of proton transported (β) or moles of water dragged per mole of hydrogen utilized (α). In this analysis, electro-osmotic drag will be consistently referred to by "α".

[1] The "electrode" is variably defined in the fuel cell literature. In this analysis, the gas diffusion layer along with the catalyst layer is defined as the electrode.

Water is produced at the cathode by the reaction between protons and oxygen ions as shown by the equation in Figure 2. The protons also drag some amount of water from the anode side. So, it can be expected that, under certain operating conditions, the concentration of water on the cathode side is higher that that on the anode side. This concentration difference causes diffusion of water from the cathode to the anode side. This is referred to as the "back-diffusion" of water. The *net* transport of water from the anode to the cathode side is the difference between the water that is electro-osmotically dragged and the water that diffuses back. The concept of "water drag" will be dealt with in more detail later.

1.4 Existing Literature

Essentially, one can view the issue of water and thermal management in automotive fuel cell systems at two levels - one; at the cell level to ensure proper membrane hydration and thereby ensure good conductivity of the membrane and two; at the fuel cell system level to keep the stack from heating up and to ensure water self sufficiency of the fuel cell system. Obviously, the requirements at one level play into the requirements at the other level. This section while giving an account of the published fuel cell literature that focuses on water and thermal management at the cell and the system level will point out the dearth of public literature in the case of WTM in automotive fuel cell systems.

Cell Level Analysis:

There have been numerous cell level studies of water and thermal management as will be shown in this section. Dawn Bernardi and co- workers at General Motors were among the first to highlight the issue of water management in PEM fuel cells. Bernardi (1990) shows a water balance calculation for a PEM fuel cell. The sensitivity of water balance to input conditions such as relative humidity is clearly illustrated in her study. However, this effort did not include a detailed membrane model. Bernardi and Verbrugge (1992) developed a unified cell model that models the anode, membrane and catalyst layers. Nevertheless, the membrane model assumed a perfectly humidified membrane.

Springer et al. (1991) at Los Alamos national labs presented a one-dimensional unified PEM fuel cell model and partially validated the results of their model with experimental data. One of the key features of this analysis was modeling of membrane behavior with respect to various operating parameters such as stream temperatures, pressure and stoichiometry. This analysis did not model the transport processes inside the catalyst layer. Springer et al. (1993 and 1996) later performed detailed modeling of transport phenomena in the catalyst layers. The latter, however, did not model the water transport in the fuel cell. They validated their models with results obtained from single cell experiments in their laboratories.

Nguyen and White (1993) presented a two-dimensional model (across the membrane and along the flow channel) of a PEM fuel cell. They model the variation in

current density, water transport, stream temperatures and pressure along the channel. They also model the effect of varying anode inlet humidity. However, they ignore the transport processes in the gas-diffusion layers and the catalyst layers. Yi and Nguyen (1998) present an advanced version of the model presented earlier. In this analysis, they include the thermal mass of the stack, account for the impact of anode and cathode pressures on water transport and investigate co-flow and counter flow configurations in the cell. However, there is no clear validation of results in both the analyses.

Fuller and Newman (1993) at UC Berkeley performed an analysis of water and thermal management of a PEM fuel cell operated on fuel reformate (a mixture of carbon dioxide and hydrogen to simulate performance in an indirect hydrocarbon fuel cell system.) using a two-dimensional model. They predict the water profile across the stack and temperature and current density variation along the length of the channel. However, the details of their modeling approach are not clear from their paper. Also, there is no clear validation of results with experimental data.

Mosdale and Srinivasan (1995) give a review of the work that has been done by Srinivasan and co-workers at Texas A&M University. They compare the modeling efforts of various groups. Different humidification strategies are discussed and their impact of the performance of the fuel cell is studied. They do not give the exact details of their modeling approach in their paper.

Amphlett and co-workers at the Royal Military College of Canada have developed PEM fuel cell models that use a combination of theoretical mechanistic models and empirical data (Amphlett[1] et al. 1995, Amphlett[2] et al. 1995). Highlighting the difficulty in exactly understanding the water transport processes in the membrane, they perform an empirical treatment of the membrane in their analysis. However, using their models, it is difficult to predict the impact of varying parameters such as anode humidification temperature, pressure and stoichiometry on water management.

There are many groups involved in developing computational fluid dynamic (CFD) models for PEM fuel cells. Some of them are: C.Y. Wang and co-workers at Pennsylvania State University (Wang et al. 2001, Um et al. 2000), Sandip Dutta and co-workers at the University of South Carolina (Dutta et al. 2001), Hongtan Liu and co-workers at the University of Miami at Coral Gables (Kazim et al. 2000, Gurau et al. 2000). The above-mentioned CFD studies are not reviewed for this thesis.

System Level Analysis:

Several groups have performed detailed analysis of water and thermal management at the system level. The author is aware that many companies that are involved in automotive fuel cell development may be involved in detailed water and thermal management work. However, for this study, only those studies that have been published in open literature (conference proceedings and refereed journals) are taken into account.

Matthew Fronk and co-workers at General Motors addressed several issues regarding PEM fuel cell systems for transportation applications (Fronk et al. 2000). They highlight the importance of thermal management while trying to maximize the performance of these systems. The issue of water recovery in the stack and the condenser is discussed and variation of water and thermal management parasitic loads (radiator and condenser loads) with variation in the cathode pressure is discussed.

Frano Barbir and co-workers at Energy Partners Inc. have studied air supply - stack interactions and highlight several interactions that will be helpful in trying to optimize fuel cell stack performance (Barbir et al. 2000, Barbir et al. 1999). They use their indigenously developed systems for analysis.

Argonne National Labs has developed a computer simulation tool, GC tool, which can be used for fuel cell system design and analysis (Geyer and Ahluwalia 1999). Their PEM fuel cell model is primarily a curve fit where the voltage is modeled as a function of current, cell temperature and the partial pressure of oxygen at the cathode inlet. They do not model the water transport processes inside the fuel cell and hence, do not take into account variable membrane hydration. They claim to be able to dynamically model the variation in stack temperature. They employ fundamental models for their condenser and heat exchangers and also have detailed pump models that model the energy consumption of the pumps.

Melanie Sadler and co-workers at Ricardo Consulting, an automotive consultant, model the thermal management requirements for a hybrid sport utility vehicle (Sadler et al. 2001). The exact details of their modeling are not clear from their papers. They claim to be developing "intelligent" cooling system designs that minimize the water and thermal management loads. They use Flowmaster® for modeling the heat exchangers.

Robert Moore and co-workers (includes the author) at University of California, Davis, as part of developing detailed fuel cell vehicle models have attempted to understand the various complex interactions that occur inside a fuel cell system and have developed methodologies to develop optimized control schemes that maximize the performance of fuel cell vehicles (Eggert et al. 2000, Badrinarayanan et al. 2000, Friedman et al. 2001, Badrinarayanan[2] et al 2001). They use a combination of fundamental and empirical models for their components. Most of the components have been validated against experimental data. However, in the context of water and thermal management, they do not quantitatively address the issue of cathode flooding in their studies.

Table 1 gives a summary of various research groups working on cell level and system level water and thermal management issues in PEM fuel cell systems.

Research Area	Research Groups
Cell Level	Los Alamos National Labs: Electronic Material Devices Group
	General Motors Corporation: Physical Chemistry Department
	Texas A&M University: Center for Electrochemical Research
	University of Kansas: Chemical Engineering
	Royal Military College of Canada, Ontario
Cell Level: CFD	Pennsylvania State University, Mechanical Engineering
	University of South Carolina: Mechanical Engineering
	University of Miami, Coral Gables: Mechanical Engineering
System Level[2]	General Motors Corporation
	Ricardo Consulting
	Nissan Motor Company
	Royal Military College of Canada, Ontario
	University of California, Davis
	Energy Partners Inc.
	Argonne National Labs (GC Tool)

Table 1: Research Groups working on Water and Thermal Management in PEM Fuel Cell Systems

[2] The author is aware that there may be many other groups involved in WTM system level work. This list mainly includes groups that have published papers at conferences or refereed journals.

2. Modeling Methodology

This section details the modeling requirements for an analysis of water and thermal management of an automotive fuel cell system. The models developed by the author for this analysis will be explained along with the model limitations.

The intention in these analyses is to fundamentally understand the processes inside the fuel cell system and thereby devise strategies to improve their performance. Hence, the models developed are mostly fundamental models that represent the physics of the processes involved. Nevertheless, for components such as the radiator, whose physics have been very well understood due to many years of research, empirical models are used to represent realistic operation.

The performance of the fuel cell system depends on various parameters, namely, the anode and cathode parameters such as pressure, stoichiometry[3] and humidity, cell operation temperature, nature of the materials used, the geometry of the components and so on. The purpose of this analysis is to understand the impact of varying these parameters on fuel cell system performance. Of more interest are those parameters that seem to increase the performance of one component at the cost of performance of another. In particular, this analysis will focus on anode saturation temperature, the cathode stoichiometry and cathode pressure. (The anode saturation temperature is the

[3] Stoichiometry in fuel cell literature is used with a slightly different meaning than in other fields. It is used as an indicator of the "excess" reactant supplied. In this study, stoichiometry means the following:
Stoichiometry = (Total number of moles of reactant supplied/ Total number of moles of reactant used)

temperature at which the anode stream is saturated with water prior to its entry into the stack). *As mentioned earlier, it should be borne in mind that the anode-centric and cathode-centric analysis are independent studies. The models and configurations of the components are different and one should refrain from making any quantitative comparisons between them.*

First, the stack model will be described followed by the radiator, condenser, air supply and humidifier models.

2.1 Stack Model

Separate cell models and stack configurations are used for the anode-centric and cathode-centric analysis. The reasons for using two different cell models are highlighted below.

A detailed model that models the water transport through the membrane is used for the *anode-centric analysis*. In a direct hydrogen fuel cell, the losses due to the anode overpotential are negligible compared to the membrane and cathode overpotential losses (Friedman and Moore 1998). Hence, the impact on the performance of the fuel cell because of the variation in anode pressure, stoichiometry and humidity is primarily because of the variation in water transport characteristics across the membrane. This model performs a simple treatment of the anode and cathode catalyst layers. It assumes the catalyst layers to be an infinitely thin plane and does not model the transport through the catalyst layers.

For the *cathode-centric analysis*, a cell model that models the cathode catalyst layer in detail is used. The cathode overpotential losses are significant in a fuel cell. The cathode pressure and stoichiometry play an important role in determining the cathode overpotential losses. The impact of variation in cathode parameters on water transport through the membrane (and hence membrane resistance) is assumed negligible compared to their impact on cathode overpotential.

Ideally, one should have a unified model that can be used for both the analyses. Due to the difficulty of capturing all the effects in one model, two models are used. The limitations of each model will be mentioned in the respective sections.

Model 1, Anode-Centric Analysis: The anode side analysis is based on an isothermal, steady-state, one-dimensional water transport model that is built along the same lines as that developed by Springer et al. (1991). Of all the studies listed in the earlier section, Springer et al. (1991) was the only study that was able to model a partially dehydrated membrane and also model the effects of anode and cathode side parameters on the membrane resistance. Hence, it was decided to go with this approach.

Assumptions:

- The modeling here includes the transport of water and reactant species across the gas diffusion layer and the membrane. (The catalyst is assumed to be a thin plane and the transport across the catalyst is not done for this analysis).

- The only voltage losses taken into account in this analysis are the resistance losses in the membrane and losses due to cathode overpotential[4].

- The impacts of cathode flooding are not considered. (Cathode flooding is a concern and has the potential to constrain the operating characteristics of the fuel cell system. The author is aware of this and will draw caveats wherever appropriate)

- The effects of the anode – cathode pressure differences on the water transport have not been modeled.

The primary inputs into the cell model include the operating current density, the anode and cathode operating conditions and the cell temperature (Table 2). The model outputs the water profile across the fuel cell in terms of the mole fraction of water, the net water dragged across the membrane, the membrane resistance and the cell voltage.

[4] The overpotential at the electrodes (anode or cathode) can be simply defined as the deviation of the electrode potential from the equilibrium value. For example, at the anode, the overpotential can be represented by the following relation:
$\eta = E - E_r$ where E_r is the equilibrium potential and η is the overpotential. As per convention, the overpotential at the anode is defined as positive and the overpotential at the cathode is defined as negative. A good description of the concept of overpotential can be found in Hamann 1998.

The modeling parameters are mentioned in Table3. Most of the cell parameters are the same as the ones employed by Springer et al. (1991). This was done so that the results of our cell model could be validated against the results of their analysis. It should also be mentioned that the membrane thickness used in this analysis, 0.0175 cm., is a slightly higher compared to the state of the art membranes.

Inputs to the Model	
Current Density (A/sq cm.)	
Anode Conditions	Anode Stoichiometry
	Anode Pressure (atm)
	Anode Humidity (Anode Saturation Temperature)
Cathode Conditions	Cathode Pressure (atm)
	Cathode Stoichiometry
	Cathode Humidity (Cathode Saturation Temperature)

Table 2: Inputs to the Cell Model for Anode-Centric Analysis

Hence, the resistance values might seem a little higher compared to other analysis that employ thinner membranes. The basic equations that govern Model 1 are shown in Appendix A1.

Parameter	**Value**
Number of Cells	440
Cell Area	750 sq.cm
Anode and Cathode Thickness	.0365cm
Membrane Thickness	.0175cm
Cell Temperature	80 C
Anode Stoic	3
Anode pressure	3atm
System Type	Load Following
Anode and Cathode Inlet Relative Humidity	100%
Peak power	Approximately 80kW (at 80 C)

Table3: Modeling Parameters for Anode-Centric Analysis

Model 2, Cathode-Centric Analysis: The analysis done for the cathode side is based on an isothermal, steady state, three-dimensional fuel cell model that is built along the same

lines as that developed by Springer et al. [1993 and 1996]. This constitutes detailed cathode catalyst layer model and the modeling of transport of the reactants through the gas diffusion layer. Dr Robert Moore and David Friedman developed this stack model at UC Davis. The stack configuration used is a PEM stack comprised of 440 cells and an active area of 370 cm^2 per cell. The stack was chosen to achieve a net peak power of approximately 80kW. It can be noticed that the active area for the two stack models are substantially different. As the membrane resistance losses were higher for the anode-centric analysis, possibly because of the high thickness of the membrane used, a higher active area was required to achieve approximately the same peak power.

Assumptions for Model 2:

1. The membrane resistance is assumed to be a constant at 0.1 ohm sq cm.

2. The net water drag ratio is assumed to be a constant at 0.2 moles of water per mole of protons transported. It is understood that the water drag can vary with changes in operating conditions (see Figure 5) and will draw caveats wherever appropriate.

The potential impacts of cathode flooding are not modeled. The exact conditions that lead to cathode flooding are unclear, but are a concern and have the potential to constrain the operating characteristics of a fuel cell system. The authors will draw caveats wherever appropriate. The basic voltage calculation equation of Model 2 is shown in Appendix A2.

2.2 Radiator and Condenser

The purpose of the vehicle radiator is to maintain the fuel cell stack temperature at around 80 degrees centigrade. For this purpose a radiator with an area of 0.5 m^2 and a variable speed fan has been modeled. The sizing of the radiator was done so that one could operate continuously at a maximum stack gross power of 80 kW with a fan output of approximately 2 kW and maintain stack temperature at 80C. The radiator model is based on a lookup table that uses empirical data generated from a standard brazed aluminum, single-pass radiator with 33 tubes (Figure 3). (personal communication with an expert[5])

The purpose of the condenser is to aid in water recovery for the system. The model of the air-air/steam condenser that is used for this purpose is based on a cross flow heat exchanger with a variable speed fan. It must be mentioned that the sizes used in the condenser model maybe somewhat arbitrary considering the dearth of data for condensers for this particular application. The model is a fundamental model and employs simple correlations for the heat transfer coefficients. As the models are fairly simple, they might not realistically represent fan loads or size, but they will be able to highlight certain trends that will be illustrated in the sections to come.

[5] Ricardo Inc., Q vs. Air Mass flow curves for modern radiator, fax received on August 21, 2000

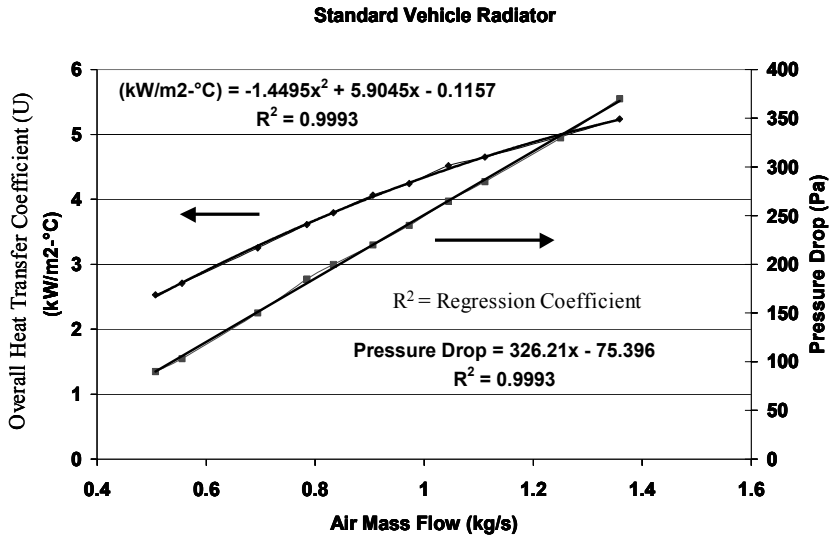

Figure 3: Standard Vehicle Radiator Characteristics

2.3 Air Supply

The air supply system is not explicitly modeled for the anode and cathode side analysis. However, the cathode conditions used in the anode side analysis are the result of a stack – air supply optimization. The optimization is simply a process of choosing an air flow rate and pressure that maximizes the efficiency of the stack at a current density, given the constraints of the stack and air supply system. Characteristic of a twin-screw device is used for the optimization.

For the anode side analysis, the cathode operating conditions, i.e. the flow rate and the operating pressures (for the cathode side) have been derived from work done earlier (Friedman and Moore 1998). These inputs arise from an optimization of the stack and air supply system and represent the operating strategy for a well-humidified stack.

The water and thermal management parasitic loads on the system have not been taken into account in the above-mentioned optimization. A typical optimized stack compressor operating control scheme (for a twin screw compressor) is shown in Figure 4. These characteristic curves will change with different air supply technologies. (Cunningham et al. 2001)

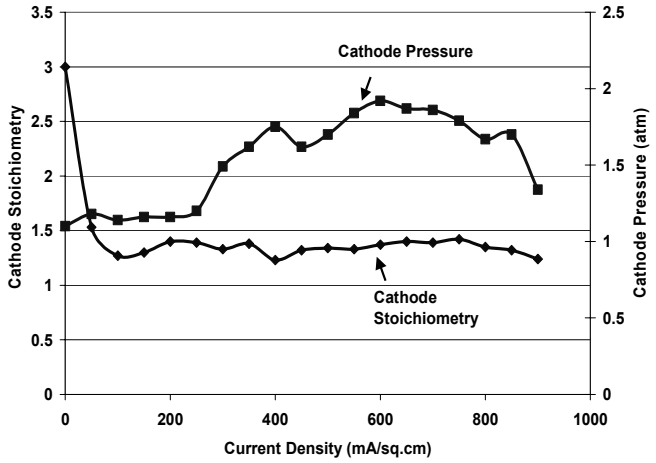

Figure 4: An Optimized Stack-Compressor Operating Control Scheme for the Anode Side Analysis

2.4 Anode Humidifier

The anode humidifier is modeled as an electric heater with 100 percent efficiency. *Note:* Other methods of humidification are possible. Wood et al. (1998) list some of the various humidification schemes that could be employed for the anode side.

3. Anode-Centric Analysis

In this section, the impact of the anode saturation temperature on the stack and system performance is studied. There are several anode side parameters such as anode pressure, stoichiometry and humidity that affect stack performance. However, while trying to study *trade-offs* between the stack and the system, the anode pressure and stoichiometry for a direct-hydrogen fuel cell system can be varied relatively independently without significant impact on system performance, except maybe for the pumping loads that are used for recirculation of hydrogen in the anode loop. However, if we take the case of anode inlet humidity, we can observe a distinct trade-off.

Several experts claim that the stack performance is enhanced when the anode saturation temperature is increased above the cell operating temperature (Prater 1994, Nguyen and White 1993, Fuller and Newman 1993, Bernardi and Verbrugge 1992). (*The anode saturation temperature is the temperature at which the anode stream is saturated with water prior to its entry into the stack.* It can be viewed as a proxy for water content of the stream.) However, this enhancement in performance comes at a price. There needs to be some heat added to the anode inlet stream to increase its anode saturation temperature. This heat has to either come from a burner or an electric heater that runs off the stack. An electric heater might seem like a more likely option in an automobile for ease of controls. This electric heater is a parasitic load on the fuel cell system. (The electric heater load ranges from about .7 kW at 13kW gross stack power to about 7kW at

70kW gross stack power for 80 C anode stream operation.) As these loads are significant, the above-mentioned trade-off has to be investigated to arrive at the optimal humidity.

3.1 Stack Level Impact of Increasing the Anode Saturation Temperature

In this section the impact of increasing the anode saturation temperature on stack performance is performed. Before getting into the analysis, it might be in place to revisit the concept of "water drag" and its significance in fuel cell operation.

Water Drag: In simple words, when the hydrogen ions travel across the membrane from the anode to the cathode, they tend to drag some water molecules with them. This phenomenon is known as "electro-osmotic" drag. The electro-osmotic drag is a result of the proton transport mechanism in the membrane. There are many studies analyzing the mechanism of proton transport and there is no single definitive mechanism that has been proposed. (Thampan et al. (2000), Eikerling and Kornyshev (2001), Ren and Gottesfeld (2001), Kreuer (2000)).

Water is produced at the cathode and some water tends to accumulate at the cathode from the electro-osmotic drag. Under most operating conditions, the concentration of water becomes higher on the cathode side than on the anode side, leading to "back-diffusion" of water towards the anode side. So, there are two components to water drag - "electro-osmotic" drag and "back diffusion". If the anode and cathode are operating at different pressures, the pressure differential can also influence the water transport process in the membrane. The effect due to the pressure differential

depends on the pressure gradient. In this analysis, the effect of pressure differential on water transport is neglected. The result of the above-mentioned competing effects is the net water dragged. In general, water drag refers to the "net water drag". The mathematics behind modeling water drag can be found in Springer et al. (1991)

As mentioned in the earlier section, in this analysis, water drag will be represented by the ratio "alpha".

Alpha = Moles of water dragged per mole of hydrogen utilized

Therefore, the net amount of water dragged across the membrane will be a product of the hydrogen utilized and alpha.

$$nH2O\_drag = nH2\_utilized * alpha \qquad \textbf{Equation 1}$$

Where *nH2O_drag* is the net water dragged and *nH2_utilized* is the hydrogen utilized at the cell.

What is the importance of water drag? The amount of water dragged can play an important role in the performance of the fuel cell. The water that is dragged across the membrane helps in keeping the membrane humidified. A membrane that is not well humidified can have high resistance leading to substantial voltage losses in the fuel cell. So, in general the anode stream and maybe also the cathode stream have to be humidified with the intention of keeping the membrane well hydrated. So, if one can achieve zero net water drag in a fuel cell, one can possibly get away without humidifying the streams (Buchi and Srinivasan 1997). Achieving net zero water drag might warrant new designs

of flow field plates and flow directions. According to Buchi and Srinivasan (1997), it is possible to operate a cell over a wide range of current densities without humidification but with a reduced performance compared to the humidified case.

The total amount of water dragged adds to the total amount of water produced at the cathode layer. So, a large water drag brings up the concern of cathode "flooding" which can substantially bring down the performance of the fuel cell. This happens because liquid water blocks the pores and thereby hinders the transport of oxygen in the cathode.

Stack Level Impact of Increasing the Anode Saturation Temperature: The stack model was run to simulate the impact of changing the anode saturation temperature above the cell operating temperature. Figure 5 shows the variation in net water drag ratio (alpha) with current density for different anode saturation temperatures. This plot has been derived for optimized cathode conditions as shown in Figure 4. (Note: Constant cathode conditions have not been maintained throughout). Constant anode conditions have been maintained (Anode Pressure =3atm. Anode Stoic =3). It can be seen that with an increase in anode saturation temperatures the amount of water dragged increases. In simple words, increasing the water content in the anode stream increases the amount of water dragged. Also, alpha was found to increase with an increase in current density. These results match well with the results in Springer et al. (1991).

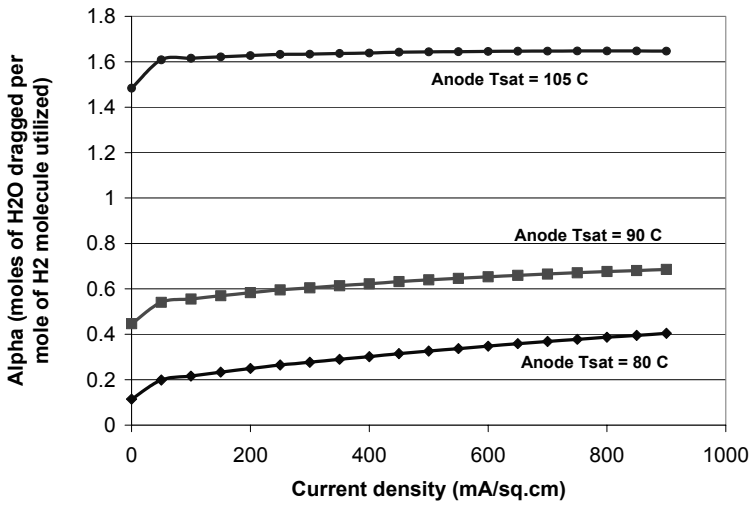

Figure 5: Variation of Water Drag with Current Density for Different Anode Saturation Temperatures

The implication of the above trends of anode saturation temperature on membrane resistance is shown in Figure 7. It can be noticed that the membrane resistance decreases with an increase in anode saturation temperatures. This can be explained by the fact that when the cell is operated at higher anode saturation temperatures, the increased water drag helps in keeping the membrane well humidified and hence decreases the resistance. However, there is a slight paradox here. It was noticed earlier that with an increase in current density the water drag ratio also increased. However, with an increase in current density, the membrane resistance is shown to increase. This seems to conflict with our earlier reasoning. The answer lies in the water profile in the membrane. So, the water drag ratio does not solely dictate the membrane resistance. The water profile in the membrane dictates the membrane resistance. Buchi and Scherer (2000) have performed an excellent study on the varying water profiles in membranes with varying current

densities. Figure 6 taken from Buchi and Scherer (2000) indicate the transverse water profile of a cell where the electrolyte is made up of four Nafion 112 sheets (Total thickness 240 μm) for different current densities. First the resistances in the four segments were measured and then these resistances were converted to membrane water content. It can be seen that the membrane segment close to the anode side has lower water content at higher current densities whereas in the other three segments, the membrane water content increases with current density. This region of low water content close to the anode side results in higher total membrane resistances at higher current densities.

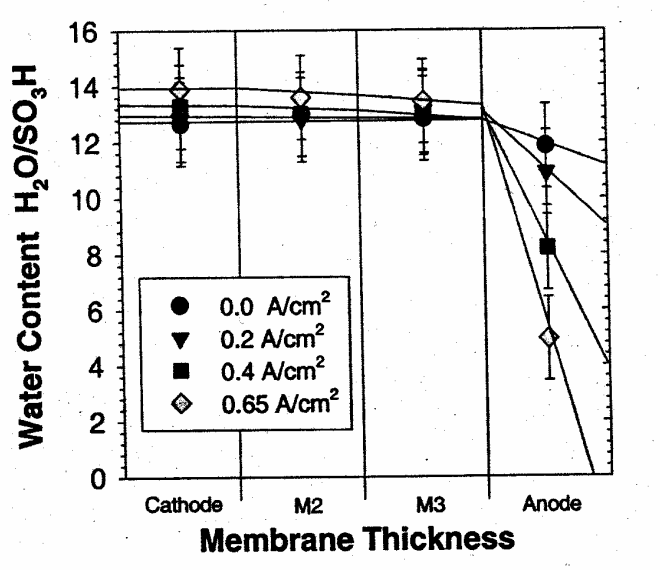

Figure 6: Transversal Membrane Hydration of Membrane in H2/O2 Fuel Cell with Four Nafion 112 Membranes at Different Current Densities. Points are Averaged Water Content in Each Membrane. Cell Temperature = 72C, Both Gases Humidified at 80 C. (Source: Buchi and Scherer 2000)

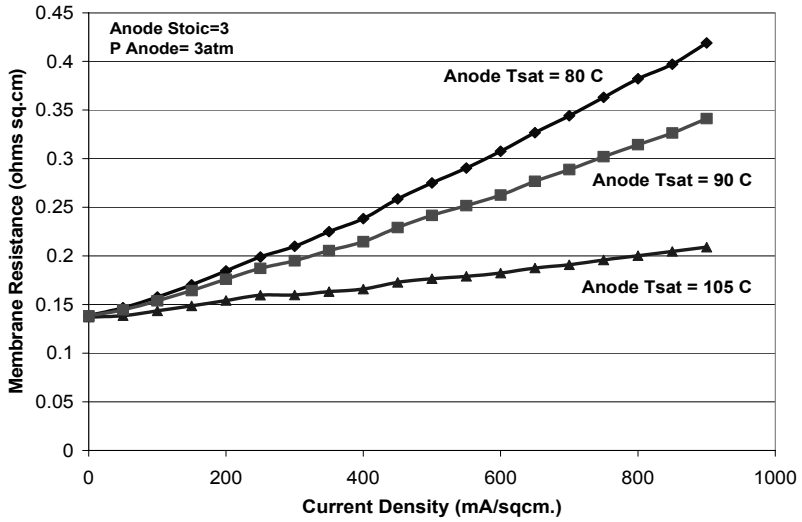

Figure 7: Variation of Membrane Resistance with Current Density for Different Anode Saturation Temperatures

A polarization plot that takes into account the resistance losses and the cathode overpotential losses is shown in Figure 8. It can be seen that the change in the voltage-current density curve with anode saturation temperature at low current densities is almost negligible. However, at higher current densities higher anode saturation temperatures yield higher voltages leading to enhanced stack performance. It can also be observed that these curves are not smooth. This is primarily because of the varying optimized cathode conditions used in this analysis. A useful way of viewing the polarization plot in Figure 8 is illustrated in Figure 9 where the stack power has been plotted against the current density. The stack power is calculated as the product of the cell voltage, number of cells, the current density and the active area.

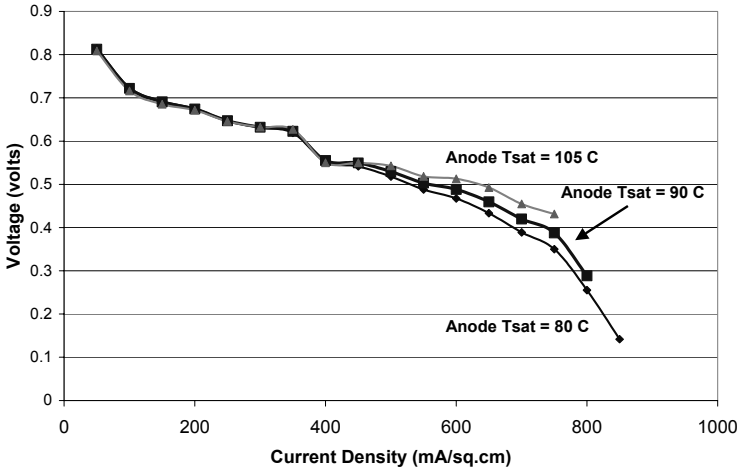

Figure 8: Polarization Curves for Different Anode Saturation Temperatures

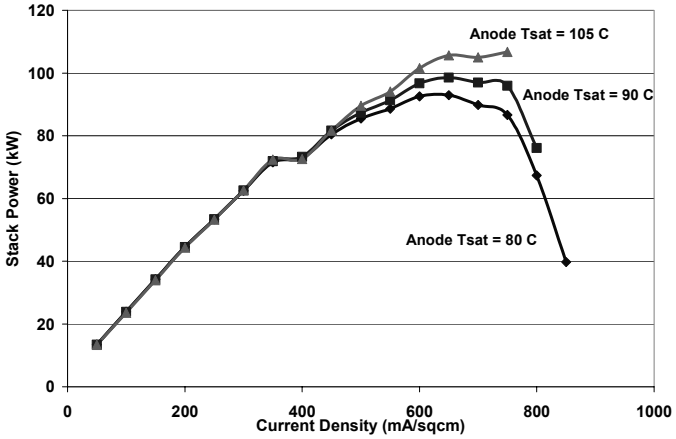

Figure 9: Power –Current Density Curve for the Stack for Different Anode Saturation Temperatures

3.2 System Level Implications of Increasing the Anode Saturation Temperature

It was shown in the previous section that an increase in anode saturation temperature enhances the stack performance. In this section, the system level impacts

of increasing the anode saturation temperatures will be analyzed. There are primarily four effects:

1. Increased Humidification Loads:

As the anode saturation temperature is increased, more water vapor is required to achieve complete saturation of the anode inlet stream. As water vapor is not readily available, liquid water (recovered from the cathode exhaust) is vaporized to meet this water requirement. In this modeling exercise, it is assumed that there is an electric heater on board that supplies the heat to vaporize the water. Another possible method of supplying the heat energy required for humidification, as mentioned earlier, would be to employ a hydrogen burner. This method offers the potential of being more efficient as the heat energy from the hydrogen can be used directly and is spared the "inefficiency" of the fuel cell. A preliminary analysis indicates that such a burner might bring down the humidification loads but does not change the trends that are being illustrated in this section.

As outlined earlier, this energy required by the electric heater is a parasitic load on the fuel cell system. A higher anode saturation temperature means a higher parasitic load as the amount of water that needs to be vaporized is higher.

The stack –power current density curve corrected for this humidification load is shown in Figure 10. The parasitic load is assumed to be equal to the

energy that is needed to vaporize the water that is dragged. The following relation gives the total amount of water dragged in the stack:

$$nH2O\_drag\_tot = nH2O\_drag * n\_cell \qquad \textbf{Equation 2}$$

Where *nH2O_drag_tot* is the total amount of water dragged in the fuel cell stack and *n_cell* is the total number of cells in the stack. A recirculation scheme is assumed on the anode side. Consequently, the water needed for humidification at any operating point is the water that is dragged at the given operating point. The following relation gives the total amount of energy required to vaporize the water:

$$P_{humidification} = nH2O\_drag\_tot * Hfg \qquad \textbf{Equation 3}$$

Where $P_{humidification}$ is the total amount of power required to vaporize the water and *Hfg* is the latent heat of vaporization of water. Model predicted values for $P_{humidification}$ at 300 mA/sq cm. are about 5.8kW at 80 C, 12.8kW at 90 C, and 34 kW at 105 C.

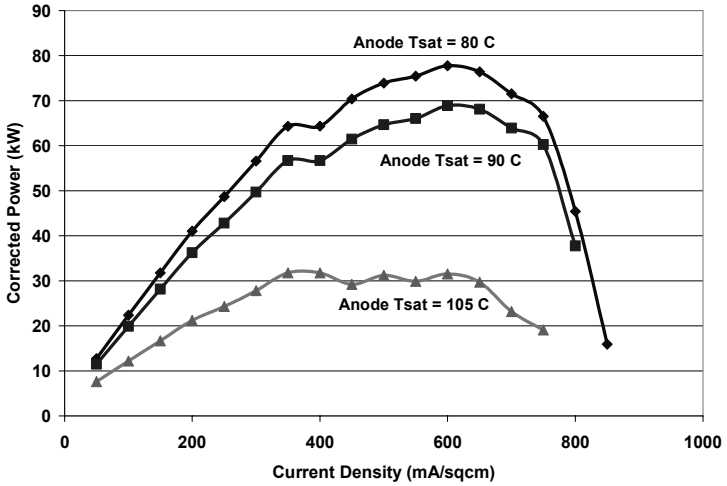

Figure 10: Power- Current Density Curve Corrected for Humidification Loads Only[6]

It can be seen in Figure 10 that the curve that corresponds to the highest anode saturation of 105 C shows the lowest net power for any given current density. Nevertheless, we have to consider all the effects before reaching any final conclusion regarding optimum anode saturation temperature.

2. Increased Stack Efficiency:

   It was observed that higher anode saturation temperatures resulted in higher cell voltages. As the stack is operating in a more efficient mode when the anode saturation temperature is increased, the amount of heat that has to be dissipated due to the inefficiency is also decreased. This can potentially decrease the radiator loads. (Just to provide a sense of magnitude of the radiator fan power: Model

[6] The air supply loads are not taken into account in these plots and hence "ups-and-downs" in the curves can be observed.

predicted radiator fan loads are in the order of about 300W for a stack gross power of 60kW.)

3. Increased Condensation Loads:

The water needed for humidification is recovered from the cathode exhaust. Some amount of water can get condensed in the stack. The remaining amount of water that is required is recovered at the condenser. The heat of condensation of the water condensed in the stack has to be rejected by the radiator. So, any condensation inside the stack increases the radiator loads. With an increase in anode saturation temperature, more water needs to be condensed, as more water is required for humidification. Therefore, two cases must be considered- 1) not all the water needed is condensed at the stack and some amount of water recovery will have to be performed at the condenser; and 2) more than the required amount of water can be condensed at the stack thereby leading to excessive heat loads on the radiator. In either case, the parasitic loads of condensation increase with an increase in anode saturation temperature as the water requirement increases. However, the magnitude of the increase depends on whether the water is condensed in the stack or the condenser.

4. Increased Radiator Loads:

The radiator loads can possibly increase because of the changes in the gas phase enthalpies when anode inlet streams with temperatures higher than the stack

temperature enter the stack. However, analysis indicates that this effect is not significant compared to the other two effects mentioned above in points 2 and 3.

Figure 11 illustrates the power-current density curve corrected not only for the humidification loads but also the radiator and condenser loads. It can be observed that the trends shown here are the same as the ones showed in Figure 10. The characteristics of Figure 11 suggest that at higher anode saturation temperatures, the gain due to improved stack performance is not able to compensate the increased humidification and radiator loads. In fact, it can be seen that the curves are a little further apart suggesting that the increase in radiator and condenser loads more than compensate the effects of increase in stack performance. So, for the given set of system parameters and for the assumed configurations of the radiator and condenser, increasing the anode humidification temperature does not enhance the system performance.

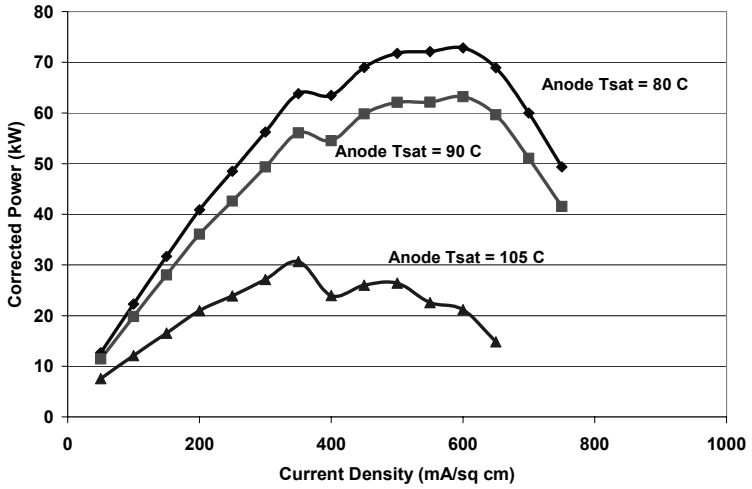

Figure 11: Power - Current Density Curve Corrected for Humidification, Radiator and Condenser Loads

3.3 Reformate Fuel Cell Operation

The above analysis has been performed for a direct hydrogen fuel cell system. The case for a reformate fuel cell system can be different. A reformate fuel cell system employs a fuel processor that processes a hydrocarbon fuel (such as methanol or any other hydrocarbon) on-board the vehicle to a hydrogen rich stream. The reformate usually exits the fuel processor at a temperature much higher than the stack operating temperature (Ramaswamy et al.2000). This heat of the reformate can be used to humidify the stream (Eggert et al. 2000). The extent to which the reformate can be humidified by using its own heat will be dictated by the composition of the reformate and its temperature at the exit of the fuel processor.

So, if the reformate fuel cell system can do away with the humidification load, then a higher anode saturation temperature may potentially lead to enhanced system performance. This prediction will have to be verified by modeling or experimentation in order to fully understand the various interactions that take place in the system.

4. Cathode-Centric Analysis

In the previous chapter, an anode centric analysis was performed. In this chapter, the importance of the cathode side parameters (pressure and flow rate) will be examined in the context of water and thermal management of a direct-hydrogen fuel cell system. This analysis illustrated in this section follows from earlier work done by the author and co-workers (Badrinarayanan et al. 2000, Badrinarayanan[2] et al. 2001)

This work will primarily deal with the analysis of a direct-hydrogen fuel cell system. For a quantitative comparison of the direct-hydrogen, indirect methanol and indirect-hydrocarbon fuel cell systems, the reader is encouraged to read Eggert (2001).

The first three sections in this chapter will discuss water recovery in a DHFC system and the effect of cathode pressure and stoichiometry on water recovery. The fourth section will examine the importance of the "shift" in water recovery brought about by increasing pressure or decreasing stoichiometry. The fifth and the sixth section will illustrate a methodology to determine the optimal cathode pressure and stoichiometry in the context of first, the WTM system and then, the overall system.

4.1 Water Recovery in a DHFC System

The water needed for the DHFC system is recovered from the cathode exhaust stream. The water in the cathode exhaust is from four different sources.

1. Water produced by the reaction between hydrogen and oxygen

2. Water used to cool and humidify the cathode

3. Net water dragged from the anode to the cathode

4. Water in the cathode due to ambient relative humidity.

Under certain operating conditions, the amount of water in the cathode of the fuel cell stack can be much more than the air stream can hold in the vapor state. This results in condensation inside the stack. Figure 12 shows the state of water in the cathode exhaust for constant cathode pressure of 0.21Mpa and a cathode stoichiometry of 1.5.

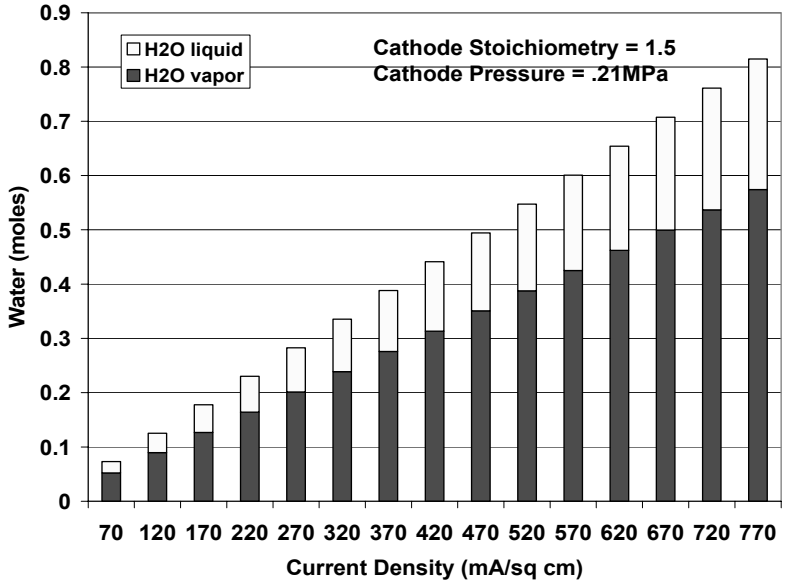

Figure 12: State of Water in the Cathode Exhaust

The cathode stoichiometry at any given operating point is defined as:

Cathode Stoichiometry = Total moles of O_2 supplied / Total moles of O_2 used

Based on the above definition, for the data shown in Figure 12, at any given current, twice the amount of oxygen needed for the reaction is supplied to the stack.

The amount of water that is condensed in the stack and recovered from the stack exit may not be sufficient to meet the system water requirements. The additional water needed is condensed from the cathode exhaust by means of a condenser. Hence, the amount of water that needs to be condensed at the condenser depends on the amount of water condensed in the stack. The following relation gives the amount of water that must be condensed in the condenser at any instant for water balance:

Condenser water recovered = System Water Required – Water Condensed in the Stack

If the water condensed in the stack exceeds the system water requirement, the condenser will not have to perform any water recovery. It will be shown in the following section that the magnitude of condensation that occurs at the stack versus in the condenser is strongly affected by the operating pressure and stoichiometry.

4.2 Impact of Cathode Pressure Variation

The analysis in this section is for the case of a constant system operating current of 216 A (600mA/sq cm). For any given operating current and constant anode conditions,

we can assume that the water requirements for the system remain relatively constant irrespective of the cathode pressure and stoichiometry[7]. Consequently, it can be assumed that for a given operating current, the total amount of water in the cathode exit also remains relatively constant irrespective of the cathode conditions. When the cathode pressure is increased while keeping the mass flow rate of air and water constant, the partial pressure of water vapor in the cathode exhaust increases up to the saturation pressure[8] (at the stack operating temperature = 80C). If the pressure is further increased, water begins to condense out of the stream. Any further increase in pressure will result in an increased condensation of water. Therefore, the amount of water that gets condensed out of the stream depends on the cathode pressure.

Figure 13 illustrates the cathode exhaust conditions for increasing pressures for a constant current of 216A (600mA/sq cm) and constant cathode stoichiometry. The white portion of the block indicates the amount of water vapor in the stream and the shaded portion indicates the amount of liquid water. As the pressure is increased from 0.15 MPa to 0.25MPa, the amount of water condensed within the stack increases. For this example, the system water requirement is shown in the plot to be around 0.1 moles/second

[7] In actuality, the system water requirements will vary slightly based on the cathode humidification requirements. The humidification requirements depend on pressure and stoichiometry. This is taken into account in the overall system analysis, but for this discussion, the relative constancy of system water requirement is a good estimation.

[8] The phenomena described here can be viewed as moving along a constant temperature line (from the right) in a typical PV diagram for water. The quality remains constant at 1 (all vapor) till the saturation pressure is reached. Once the partial pressure of water is increased beyond the saturation pressure, water starts to condense out.

(horizontal black line). If instantaneous water neutrality is to be achieved, the net water that needs to be recovered from the cathode exhaust at this operating current is also 0.1 moles. The condenser needs to condense the difference between 0.1 moles/sec and the amount of liquid water condensed inside the stack (in case the water condensed in the stack is not sufficient to meet the system water requirements). As shown in Figure 13, as the pressure increases, the amount of water that must be condensed at the condenser decreases. It can be seen that at a pressure of 0.25MPa, the water recovered in the stack exceeds the system water requirement at that instant.

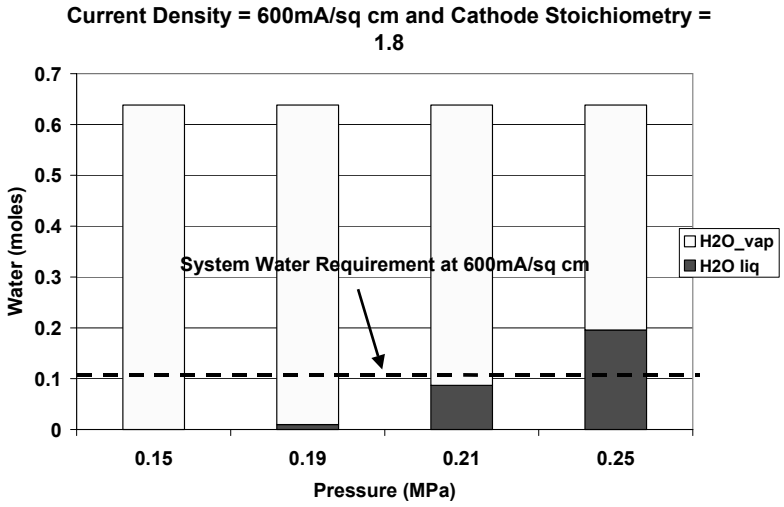

Figure 13: Cathode exhaust conditions for varying cathode pressures and a constant stoichiometry of 2

4.3 Impact of Cathode Stoichiometry Variation

A similar analysis can be performed for the cathode stoichiometry. The analysis in this section is being done for the case of a constant system operating current. Similar to

the discussion on pressure, it can be assumed that for a given operating current, the total amount of water in the cathode exit remains relatively constant irrespective of the cathode conditions. Figure 14 illustrates the state of water in the cathode exhaust for varying stoichiometry for a constant current of 216A (600mA/sq cm) and a constant pressure. The "white" portion of the block indicates the amount of water vapor in the stream and the "shaded" portion indicates the amount of liquid water. As the cathode stoichiometry increases, the amount of water condensed inside the stack decreases. With an increase in stoichiometry while maintaining the pressure, the mole fraction of water decreases and more water can be "accommodated" in the vapor state. (With an increase in stoichiometry, the amount of water in cathode stream remains the same, but there is an increase in the amount of oxygen and nitrogen components. *Note:* For the cathode-centric analysis, there is no water (liquid or vapor) injection into the cathode stream). Water condenses in the stack as long as the partial pressure of water vapor is equal to the saturation pressure. Water condensation stops as soon as the partial pressure of water vapor drops below the saturation pressure.

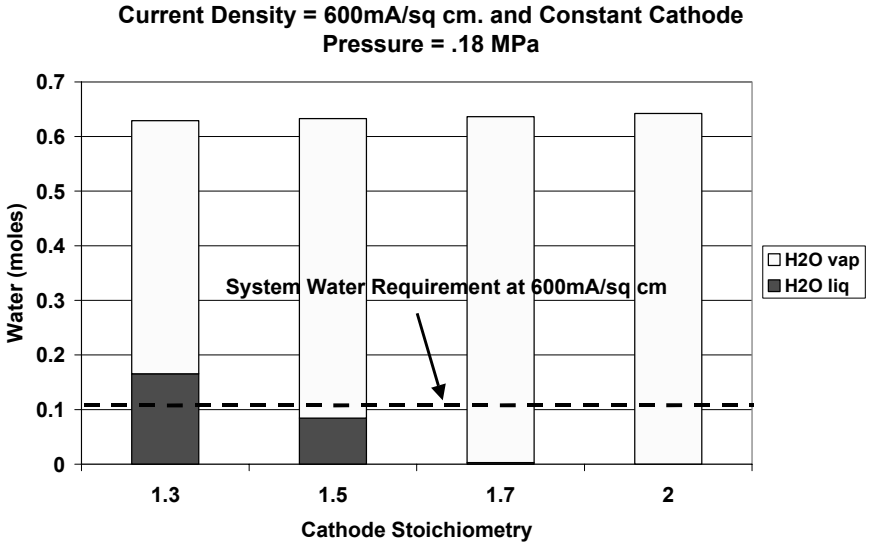

Figure 14: Cathode exhaust conditions for varying cathode stoichiometries and a constant pressure of 0.2 MPa

From Figure 14 it can be seen that the water requirement of the system is about 0.1 moles per second (horizontal black line). As the cathode stoichiometry increases, the amount of water that needs to be condensed at the condenser increases. The condenser needs to condense the difference between 0.1 moles and the amount of liquid water condensed inside the stack. If the water condensed in the stack exceeds the system water requirement, then the condenser will not have to perform any water recovery.

By varying the cathode side parameters, namely, the cathode stoichiometry and the cathode pressure, one can bring about a "shift" in water recovery from the condenser to the stack. A thermodynamic analysis of this "shift" is done in the next section.

4.4 "Shift" in Water Recovery from Condenser to Stack

The system level impact of the "shift" in water recovery from the condenser to the stack is analyzed in this section. The equations given in this section are simplified and are meant purely for discussion purposes. The actual condenser and radiator models include the more detailed analysis mentioned earlier.

At any given instant, let the total heat rejected by the system just to condense the water required by the system be equal to Q_{cond} (watts). When the cathode conditions are such that condensation occurs within the stack, some amount of this *condensation duty* is rejected at the stack and some of it is rejected at the condenser.

$$Q_{cond} = Q_{radiator\_cond} + Q_{condenser} \qquad \textbf{Equation 4}$$

Where, $Q_{radiator\_cond}$ is the heat rejected at the stack only due to condensation ($Q_{radiator\_cond}$ does not include the heat that has to be dissipated because of the inefficiency of the stack) and $Q_{condenser}$ is the heat rejected at the condenser.

Now, a new term that will be used in this analysis is defined- the required "heat rejection requirement" (HRR) for condensation of the system[9]. This variable will aid in thermodynamically understanding the "shift" in water recovery from the condenser to the stack.

[9] This analysis has been performed along the same lines as the work on 'heat rejection capacity' described in Fronk et al (2000) and many of our conclusions are similar to the ones arrived therein.

$$HRR = \frac{Q_{radiator\_cond}}{T_{Stack} - T_{amb}} + \frac{Q_{condenser}}{T_{Sat} - T_{amb}} \qquad \textbf{Equation 5}$$

Where, HRR can be viewed as the "cost" of attaining water neutrality in the fuel cell system. For the radiator, the temperature driver could be approximated to T_{stack} (stack temperature) minus T_{amb} (ambient air temperature) (Fronk et al. [2000])[10]. If there is any condensation load for the condenser, the condenser must cool the cathode exit stream from the stack temperature (assuming cathode stream to equilibrate to approximately the stack temperature) to the saturation temperature at which all the necessary water has been condensed. Therefore, for the condenser, a good estimator for the temperature driver is T_{sat} (at outlet temperature of the condenser) minus T_{amb}. T_{sat} will always be less than T_{stack} ***if*** there is a condensation requirement on the condenser. One of the simplifications in this discussion is the use of the above-mentioned ΔT's instead of ΔT_{LM}'s (log-mean temperature differences). It is important to note that these temperature drivers are approximations used in this section to aid in easier understanding and are not used in the detailed modeling.

Equation 5 can be rewritten as follows.

$$HRR = Us * As + Uc * Ac \qquad \textbf{Equation 6}$$

Where, Us, Uc, As, Ac are the heat transfer coefficients (required for condensation) and the heat transfer areas of the stack and condenser respectively. *So, HRR for condensation*

[10] Actually, the temperature driver would be the difference between the temperature of the coolant and the ambient temperature. This temperature difference is less than the one described and is what is used for the rest of the analysis. Nevertheless, for the sake of simplicity, the stack temperature is considered a close approximation in this discussion.

can be interpreted as a product of the heat transfer coefficients and the area. It must be understood that a decrease in "HRR" can result in a decreased heat transfer area or decreased heat transfer coefficient required. A lower required heat transfer coefficient might allow lower air mass flow rates and hence lower fan power.

This point has to be carefully understood. It can be seen that there is a heat exchanger size (area) versus fan power trade-off. The implication of the trade-off is that a lower HRR can result in either a smaller heat exchanger sizes or lower fan powers. What this also tells is that one could get away with a smaller heat exchanger while paying the price in terms of fan power. *A lower required HRR is "good" for the system*. As mentioned earlier, the HRR can be viewed as the "cost" of attaining water neutrality in the fuel cell system.

When the temperature of the cathode stream inside the stack is below the saturation temperature of water in the stream, condensation occurs within the stack. Once this condition is satisfied, and there is a shift in condensation from the condenser to the stack either because of an increase in cathode pressure or a decrease in cathode stoichiometry, the stack has to reject more heat. The load on the radiator increases and the load on the condenser decreases as shown by Equation 7:

$$HRR_{new} = \frac{Q_{radiator\_cond} + x}{T_{Stack} - T_{amb}} + \frac{Q_{condenser} - x}{T_{Sat}' - T_{amb}} \qquad \textbf{Equation 7}$$

Where HRR_new is the new heat rejection requirement and "x" is the shift of heat load from the condenser to the stack, as the stack has to reject more heat now. For a constant water requirement, the condenser is now required to condense less water. Under the

conditions where water is required to condense within the condenser, ($T_{sat'} - T_{amb}$) is less than ($T_{stack} - T_{amb}$) and HRR_{new} will be less than HRR. In general, shifting the condensing load from the condenser to the stack brings down the required HRR, since T_{stack} is always greater than T_{sat}.

For a lower water requirement, the new temperature that the condenser is required to condense to ($T_{sat'}$) is greater than the original T_{sat}. As the pressure increases or stoich ratio decreases $T_{sat'}$ approaches T_{stack} thereby leading to diminishing gains from the shift mentioned above.

Additionally, it turns out that when the load on the stack goes up by "x", the condenser load decreases by more than "x". This is because the condenser is required to cool not just the water vapor in the cathode exhaust, but also the residual nitrogen and oxygen. The increase in the "temperature driver" of the condenser reduces this cooling requirement as well. This effect continues as long as pressure is increased causing a further reduction in *HRR*.

4.5 Finding the Optimal Cathode Pressure and Stoichiometry

The optimization performed here is done under steady state conditions. As a result, the heat load on the radiator (radiator duty) at any current is calculated by a combination of the heat due to the inefficiency of the stack at that instant and the heat load associated with the condensation of the water inside the stack. Ignoring water condensation for the moment, the heat load on the cooling system is then a direct function

of the operating efficiency of the stack alone – the higher the stack efficiency, the less energy that must be dissipated to ensure constant temperature operation. The heat that has to be rejected by the stack due to inefficiency can be calculated by subtracting gross power from the product of lower heating value of hydrogen and the mass flow rate of hydrogen utilized at that given instant as shown in equation 8.

$$m\_dot\_H_2 * LHV_{H2} - P_{gross} = Q_{stack\_ineff} \qquad \textbf{Equation 8}$$

Where $m\_dot\_H_2$ is the amount of hydrogen utilized, LHV_{H2} is the lower heating value of hydrogen, P_{gross} is the total electric power drawn from the stack at that instant and Q_{stack_ineff} is the total amount of heat that has to be rejected by the stack due to inefficiency. In our model, this heat must be entirely rejected by the radiator and associated fan.[11]

As shown in the previous section, the power required to recover the needed water is a function of the operating conditions of the cathode since the water needed for the system is condensed from the cathode exhaust stream. As water is condensed both in the stack and the condenser, the power associated with water recovery is a combination of the added radiator fan and pump power (see Figure 1) and the fan power for the condenser – though the fan power dominates in each component. The total amount of heat that has to be rejected due to condensation of water in the stack can be determined

[11] Ambient heat loss from the stack is not considered. Also, it is assumed that the radiator fan is required to provide all the air required to remove the heat from the radiator (i.e., no allowance is made for ram-air cooling effect).

by calculating the product of the total amount of water condensed inside the stack and the latent heat of vaporization of water as shown in equation 9.

$$Q_{radiator\_cond} = Hfg * m\_dot\_H2Ostack \quad \textbf{Equation 9}$$

Where $Q_{radiator\_cond}$ is the heat that has to be rejected by the stack due to the condensation inside the stack, *Hfg* is the latent heat of vaporization of water and *m_dot_H2Ostack* is the total amount of water condensed inside the stack at that given instant.

Now, the total radiator load can be arrived at by simply adding the Q_{stack_ineff} and $Q_{radiator\_cond}$ as shown in Equation 10.

$$Q_{rad\_tot} = Q_{radiator\_cond} + Q_{stack\_ineff} \quad \textbf{Equation 10}$$

A "Water and Thermal Management (WTM) only" optimal operating strategy is developed ignoring the possible effects of cathode flooding. Figure 15 and Figure 16 illustrate the characteristics of the WTM sub-system for varying air pressure and varying air flow respectively. Each figure shows the power required by the total WTM sub-system and each component. The radiator power shown is associated with the removal of the heat required to keep a constant stack temperature plus any heat of condensation. The condenser power is that associated with condensing the remaining water necessary to ensure water neutrality within the system.

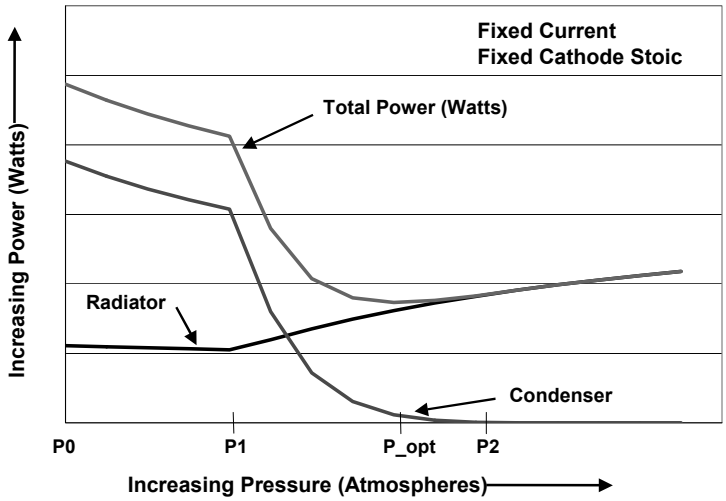

Figure 15: Effect of Pressure on the WTM Sub-system Power Requirements

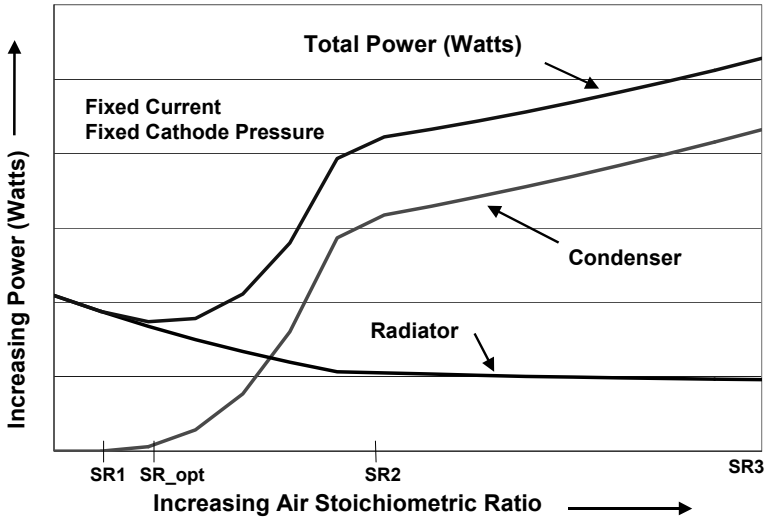

Figure 16: Effect of Air Stoichiometric Ratio on the WTM Sub-system Power Requirements.

Given a fixed current, fixed anode conditions, and a constant air-side stoichiometric ratio, Figure 15 qualitatively illustrates that an optimal operating pressure,

P_opt, can be found to minimize the total power consumption of the WTM sub-system. This optimal operating point results from the progression of factors highlighting the interactions between the air supply and the condenser and radiator discussed below.

- As the cathode pressure increases, the saturation temperature increases. Consequently, with an increase in pressure the required water condenses out at higher temperatures in the condenser. Thus, the increasing saturation temperature decreases the condenser fan power with increasing cathode pressure (The lower the temperature drop in the condenser the lower the condenser loads). This effect continues as long as there is still water to be removed in the condenser.

- For the radiator, the load decreases gradually from P0 to P1. This is due to the fact that as the pressure of the air supplied to the stack is increased, the partial pressure of the oxygen is increased at the catalyst sites, reducing the cathode overpotential and increasing the stack efficiency accordingly. This increase in stack efficiency with increasing pressure is true for the entire graph, however with diminishing returns (Friedman et al. 2001). Up to point P1, all of the water required for the system is condensed within the condenser and the radiator load accommodates only the heat rejection due to the efficiency losses in the stack. When the cathode exit pressure reaches P1, under the given conditions, liquid water begins to condense within the stack. This condensation within the stack increases the radiator duty and parasitic load as shown. Assuming this water can be effectively collected, it also reduces the parasitic load of the condenser. Thus,

above P1, the condenser load decreases due to the benefits of higher pressure and the reduced water requirement.

- As the stack benefits from a larger driving force – as discussed in the section on shifting the condensation load to the stack – the decrease in condenser fan power exceeds the increase in radiator parasitic load up until P_opt. Additionally, with an increasing required saturation temperature at the condenser exit, the effect of nitrogen and oxygen cooling is reduced as well. The result is a net decrease in the total power draw from the WTM sub-system. Therefore, purely from a WTM standpoint (and ignoring the possibility of cathode flooding), Figure 15 indicates a benefit in shifting the condensing load from the condenser to the stack and operating the system at higher cathode pressures up to P_opt. This conclusion agrees with the findings of other authors in this area (Badrinarayanan et al. [2000], Fronk et al. 2000, Barbir [1999]). However, this benefit only continues up to the point when nearly all of the water is condensed at the stack (P_opt). After this point, almost no water is being condensed within the condenser and its power has nearly reached zero – no longer providing any reduction in load with increasing pressure. Further increases in pressure above P2 simply increase the radiator parasitic load by condensing un-needed water within the stack.

Similar trends seen for variations in pressure are also illustrated in Figure 16 for stoichiometry. As with operating pressure, an optimal stoichiometric ratio is found and results from similar tradeoffs within the WTM sub-system.

Starting from SR3 and reading the graph from right to left, as SR[12] decreases, the partial pressure of the water vapor in the cathode exhaust increases. This increases the saturation temperature, resulting in a decrease in condenser parasitic load (SR3 to SR1) and an increase in radiator load due to condensation within the stack (SR2 to SR1). The other effect of SR on the radiator is the effect of the partial pressure of oxygen at the catalyst. As SR is decreased, the partial pressure of oxygen at the catalyst is reduced, giving higher cathode overpotential, lower efficiency, and increased cooling loads. These combined effects lead to a decrease in WTM sub-system power as the air flow is decreased and the condensation load is shifted more and more to the cooling system (radiator). A similar optimum is found, SR_opt where the WTM parasitic loads are a minimum. Beyond SR1, the condenser no longer provides any significant assistance and the stack begins to condense un-needed water.

In general, it can be said that from a "WTM only" perspective, high-pressure operation is generally favored, but excess pressure leads to over condensation of water. Further, lower airflow operation is also generally favored, but with a similar limit. The result is an inclination to operate at some P_opt and SR_opt in order to minimize WTM parasitic power requirements given a fixed current and anode conditions.

There are two important issues here. Firstly, at lower air stoichiometries, there is a fear of "flooding" the cathode. The issue of flooding is not explicitly dealt with in this analysis. This is an important issue that will potentially constrain the above-mentioned optimization. Secondly, low stoichiometries may not be achievable due to flow

[12] SR = Stoichiometric Ratio

constraints in the stack (Personal communication with experts[13]). This can also impose constraints on the optimization process mentioned above.

Now, in the context of optimizing the cathode conditions for the overall system, there are two questions that should be asked 1) Are the optimal cathode conditions mentioned above realistically achievable and 2) How will the above-mentioned conditions change if the stack and air supply system operation (a compressor or blower) is taken into account? The next section attempts to answer these questions and at the same time provides an example quantitative proposal for an optimal operating scheme for the cathode side.

4.6 System Optimization: Devising Optimal Cathode Conditions

While trying to optimize the performance of a fuel cell system, one attempts to maximize the net power of the system based on controllable operating parameters. In this section, an illustration of how one can go about devising optimal control strategies for the cathode side is outlined. Ideally, one would have to perform a "complete" optimization that would include the anode and cathode parameters as the fuel cell performance is influenced by both of them. This is tricky considering the difficulty of capturing all the effects in a single model. The water transport (and hence the membrane resistance) is influenced by both the anode and cathode parameters. This prevents the "independent"

[13] Discussions at the Fuel Cell Vehicle Technology Conference, UC Davis, July 2001

optimization of any one side. However, if some assumptions can be made regarding water transport across the fuel cell, such as a constant water drag ratio (alpha), one can proceed to optimize the cathode side of the fuel cell alone. (In reality, for a constant anode saturation temperature of 80 C, the water drag ratio (alpha) usually varies from 0.1 to 0.4 or depending on the current density. See Figure 5)

An equation for the cathode optimization that includes the major system components is shown in Equation 11.

$$P_{net}(\mathrm{Pr}_{air,}\, \dot{m}_{air}) = (P_{stack\_gross}(\mathrm{Pr}_{air,}\, \dot{m}_{air}) - P_{air\_system}(\mathrm{Pr}_{air,}\, \dot{m}_{air}) - P_{radiator}(\mathrm{Pr}_{air,}\, \dot{m}_{air}) - P_{condeser}(\mathrm{Pr}_{air,}\, \dot{m}_{air}))$$

Equation 11

As shown in the above relation, the operation of the stack, the air supply system and the water and thermal management system are all functions of cathode pressure and mass flow rate. While trying to devise optimal operating schemes (for the cathode side) for the system, the intention is to determine a pressure ratio and mass flow rate that maximizes the P_{net_opt} mentioned above.

Figure 17 shows optimized operating pressure control schemes for the DHFC system with a twin-screw compressor as the air supply system. The curve depicts an optimized operating control scheme that takes into account the stack, air supply system and the WTM components. To understand these curves, one will also need to recognize

the importance of the air supply - stack interactions. Discussion of air supply – stack interactions is beyond the scope of this thesis. The reader is encouraged to read Friedman et al. (2001) and Cunningham et al. (2001) for a more detailed description of the air supply interactions.

In a similar way to the optimized pressure control scheme, optimized operating control schemes can be developed for the stoichiometry. Figure 18 shows an optimized operating control scheme for stoichiometry for a DHFC system with a twin-screw compressor. The curve shows an optimized operating control scheme that takes into account the stack, the air-supply system components, and the WTM components.

Note: The water and thermal management sub-optimization analysis that contributes to the cathode optimization process is part of this thesis. However, the "complete" cathode optimization process detailed in this section is not part of this thesis. It has been included here for the sake of completeness.

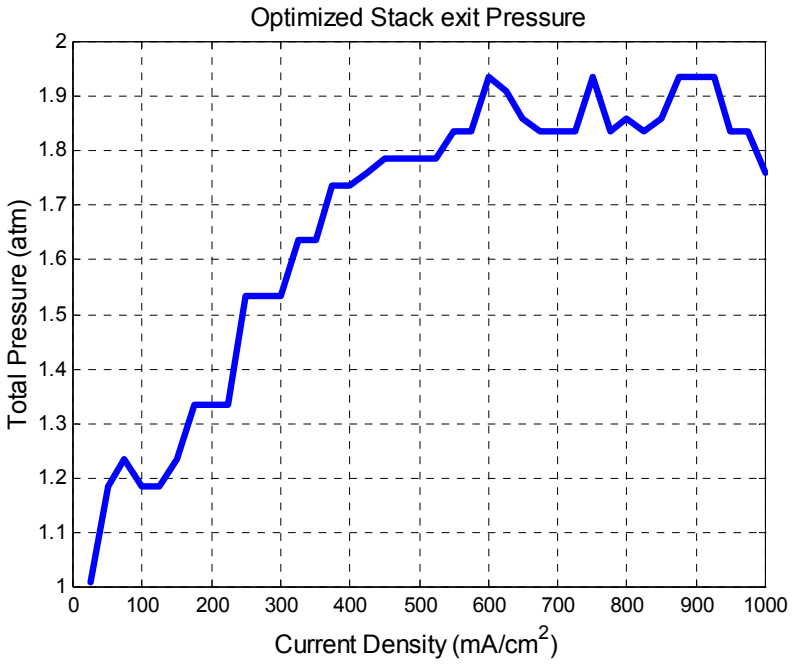

Figure 17: Optimized Cathode Pressure Operating Control Scheme (For optimized Stoichiometry, see Figure 18)

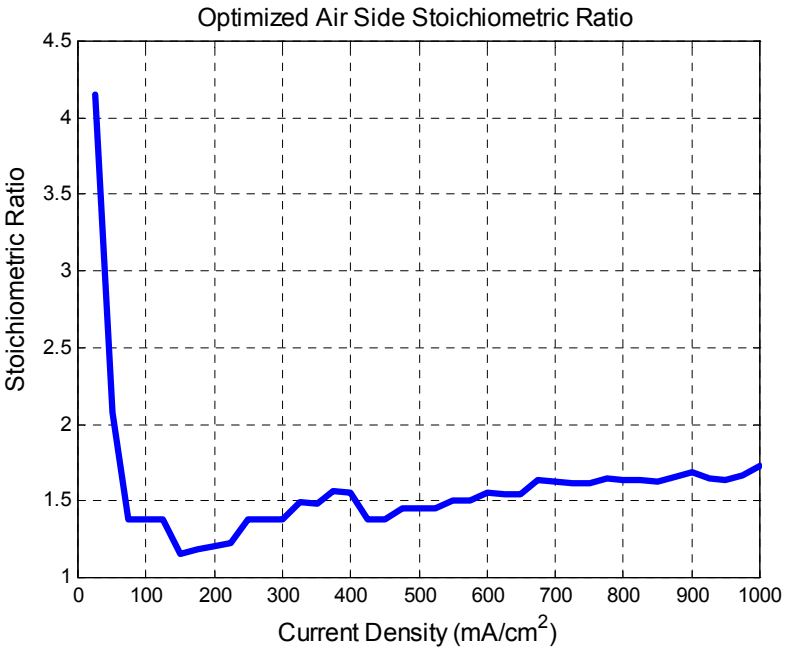

Figure 18: Optimized Cathode Stoichiometry Operating Scheme (For Optimized Pressure, see Figure 17)

It is also important to note that the position of the optimal pressure and stoic ratio is strongly influenced by the size and design of the stack, WTM, and air supply components. Increasing or decreasing the size or heat transfer coefficient of the radiator or condenser, as well as changing the operating characteristics of the air supply is likely to shift the optimal operating points. It becomes clear that sizing of the components in the system is also part of the overall optimization process.

5. Conclusions

Water and Thermal Management is one of the key technical issues that have to be well understood in the process of fuel cell system development. As shown earlier, there is a dearth of published literature in this area.

One of the primary objectives of this thesis was to illustrate a methodology to recognize the various interactions in a fuel cell system *in the context of water and thermal management*. The modeling tools that would be required for such an analysis are described. Tools (i.e.; models) were developed for a load following direct hydrogen fuel cell vehicle primarily using fundamental representation of the physical processes that occur inside the fuel cell system. The models were set up such that the impact of varying a single fuel cell system parameter could be studied. A set of illustrative example analyses was performed to highlight the complex interactions taking place inside the fuel cell system.

Specifically, the impacts of varying three parameters on fuel cell system operation are studied. They are the anode saturation temperature, the cathode pressure and the cathode stoichiometry. The important conclusions are as follows:

- It is shown that though there might be a benefit in stack performance by increasing the anode saturation temperature above the cell operating temperature, there may not be any gain in system performance.

- The impact of cathode operating conditions (pressure and stoichiometric ratio) can have complex and sometimes non-intuitive impacts on the water and thermal management parasitic loads of a direct hydrogen fuel cell system. Increasing cathode pressure or decreasing cathode stoichiometry can "shift" water recovery from the condenser to the stack thereby potentially decreasing the water and thermal management parasitic loads.
- It is also observed that in the case of the radiator and condenser, that heat exchanger size could be traded-off with fan power and vice versa. This should be taken into account in a full optimization.
- Though it is recognized that understanding these complex interactions is an essential step towards devising optimal control schemes for the overall system, it is not sufficient. The determination of the optimal operating points for the cathode warrants an understanding of the competing interactions between all the components in the fuel cell system, not just the WTM components.

Limitations and Future Work:

- Though this study has mostly used validated components model for the analysis, the overall system results need to be validated.
- The issue of flooding is not explicitly dealt with in the modeling. It is understood that flooding may potentially constrain the operation of the fuel cell under certain conditions. These constraints can potentially impact the determination of the

optimal control schemes. Work is currently underway to develop tools that can model the effects of flooding.

- The anode side analysis employed a one-dimensional water transport model. It is recognized that several parameters change along the flow channels and a one-dimensional analysis can potentially miss certain characteristics. This necessitates a two-dimensional analysis of the problem. Work is currently underway to develop a “segmented” two-dimensional model.

References

(In alphabetical order)

1. Amphlett[1], J., Baumert, R.M., Mann, R., Peppley, B.A., Roberge, P.R. and Harris, T.J., "Performance Modeling of Ballard Mark IV Solid Polymer Electrolyte Fuel Cell 1. Mechanistic Model development", Journal of the Electrochemical Society, Vol. 142, No.1, 1995.

2. Amphlett[2], J., Baumert, R.M., Mann, R., Peppley, B.A., Roberge, P.R. and Harris, T.J., "Performance Modeling of Ballard Mark IV Solid Polymer Electrolyte Fuel Cell II. Empirical Model Development", Journal of the Electrochemical Society, Vol. 142, No.1, 1995.

3. Amphlett, J., Mann, R., Peppley, B.A., Roberge, P.R., Rodrigues, A., "A Model Predicting Transient Responses in Proton Exchange Membrane Fuel Cells", Journal of Power Sources, Vol. 61, pp 183-188, 1996.

4. Badrinarayanan, P, Eggert, A. and Hauer, K., "Implications of Water and Thermal Management Parameters in the Optimization of an Indirect Methanol Fuel Cell System", Proc. of the 35th Intersociety Energy Conversion Engineering Conference, American Institute of Aeronautics and Astronautics, Vol. 2, pp. 1359-1366, 2000.

5. Badrinarayanan[1], P., Ramaswamy, S., Eggert, A., and Moore, R.M., "Fuel Cell Stack Water and Thermal Management: Impact of Variable System Power Operation", Fuel Cell Power for Transportation 2001, Proc. of the SAE 2001 World Congress, pp. 53-60, 2001.

6. Badrinarayanan[2], P., Eggert, A. and Moore, R.M., "Minimizing the Water and Thermal Management Parasitic Loads in Fuel Cell Vehicles", International Journal of Transport Phenomena, 2001 (Accepted).

7. Barbir, F., AES, Vol. 39, pp. 305-315, 1999.

8. Barbir, F., Fuchs, M., Husar, A., Neutzler, J., "Design and Operational Characteristics of Automotive PEM Fuel Cell Stacks", Fuel Cell Power for Transportation 2000, Proc. of SAE 2000 World Congress, pp. 63-70, 2000.

9. Bauen, A., and Hart, D., "Assessment of Environmental Benefits of Transport and Stationary Fuel Cells", Journal of Power Sources, Vol. 86, pp 482-494, 2000.

10. Bernardi, Dawn, "Water Balance Calculations for Solid Polymer Electrolyte Fuel Cells", Journal of the Electrochemical Society, Vol. 137, No. 11, pp 3334-3350, 1990.

11. Bernardi, D and Verbrugge, M., "A Mathematical Model of the Solid Polymer Electrolyte Fuel Cell", Journal of the Electrochemical Society, Vol. 139, No.9, pp 2477-2491, 1992.

12. Bird, B., Stewart, W., Lightfoot, E., *Transport Phenomena*, John Wiley and Sons, Inc., Wiley International Edition, 1960.

13. Buchi, F., and Srinivasan, S., "Operating proton Exchange Membrane Fuel Cells Without External Humidification of the Reactant Gases", Journal of the Electrochemical Society, Vol. 144, No.8, pp 2767-2772, 1997.

14. Buchi, F and Scherer, G., "Investigation of Transversal Water Profile in Nafion Membranes in Polymer Electrolyte Fuel Cells", Journal of the Electrochemical Society, Vol. 148, No.3., pp A183-188, 2001.

15. CARB, *Proposed Amendments to the California Zero Emission Vehicle Program Regulations*, December 2000.

16. Cunningham, J. M., Hoffman, M., and Friedman, D., "A Comparison of High Pressure and Low-Pressure Operation of PEM Fuel Cell Systems", Fuel Cell Power for Transportation 2001, Proc. of the SAE 2001 World Congress, pp. 61-68, 2001.

17. Dutta, S., Shimpalee, S., Van Zee, J.W., "Numerical Prediction of Mass-Exchange Between Cathode and Anode Channels in a PEM Fuel Cell", Intl. Journal of Heat and Mass Transfer, Vol. 44, pp 2029-2042, 2001.

18. Eggert[1], A, Badrinarayanan, P., Friedman, D. and Cunningham, J., "Water and Thermal Management of an Indirect Methanol Fuel Cell System for Automotive Applications", Proc. of the 2000 ASME International Mechanical Engineering Congress and Exposition - Heat Transfer Division, Ed. J.H. Kim, The American Society of Mechanical Engineers, New York, Vol. 1, pp 35-42, 2000.

19. Eggert[2], A: Thesis titled, "Water and Thermal Management of Fuel Cell Systems: Impact of Variable System Characteristic on WTM Parasitic Loads", University of California, Davis, 2001.

20. Eikerling, M., Kornyshev, A.A., "Proton Transfer in a Single Pore of a Polymer Electrolyte Membrane", Journal of Electroanalytical Chemistry, Vol. 502, pp 1-14, 2001.

21. Friedman, D.J and Moore, R.M., "PEM Fuel Cell System Optimization", Proceedings of the Second International Symposium on Proton Conducting

Membrane Fuel Cells II, Edited by S. Gottesfeld et al., Electrochemical Society, Pennington, NJ, 1998.

22. Friedman, D. J., Eggert, A., Badrinarayanan, P., and Cunningham, J., "Balancing Stack Output, Air Supply, and Water and Thermal Management Demands for an Indirect Methanol Fuel Cell System", Fuel Cell Power for Transportation 2001, Proc. of the SAE 2001 World Congress, pp. 37-46, 2001.

23. Fronk, M.H., Wetter, D.L., Masten, D.A., Bosco, A., "PEM Fuel Cell System Solutions for Transportation", Fuel Cell Power for Transportation 2000, Proc. of SAE 2000 World Congress, pp. 101-108, 2000.

24. Fuller, T., and Newman, J., "Water and Thermal Management in Solid-Polymer Electrolyte Fuel Cells", Journal of the Electrochemical Society, Vol. 140, No.5, pp 1218-1225, 1993.

25. Geyer, H.K., Ahluwalia, R.K., "GC Tool for Fuel Cell System Design and Analysis: User Documentation", Argonne National Labs, Report No. ANL-98/9, 1998.

26. Gottesfeld, S and Zawodzinski, T., "Polymer Electrolyte Fuel Cells", Advanced in Electrochemical Science and Engineering, Volume 5, Ed. by Richard C. Alkire, Heinz Gerischer, Dieter M. Kolb, Charles W. Tobias, 1997.

27. Gurau, V., Liu, H., Kakac, S., "Two-Dimensional Model for Proton Exchange Membrane Fuel Cells", AIChE Journal, Vol. 44, No. 11, pp 2410-2422, 1998.

28. Hamman, C., Hamnett, A., Vielstich, W., *Electrochemistry*, Wiley-VCH, pp 145-146, 1998.

29. Heywood, John, *Internal Combustion Engine Fundamentals*, Mc-Graw Hill, Inc., 1988.

30. Kalhammer, F., Prokopius, P., Roan, V., and Voecks, G., "Status and Prospect of Fuel Cell Engines as Automobile Engines", Prepared for the California Air Resources Board, July 1998.

31. Kazim, A., Liu, H.T., Forges, P., "Modeling of Performance of PEM fuel Cells with Conventional and Interdigitated Flow Fields", Journal of Applied Electrochemistry, Vol.29, pp 1409-1416, 1999.

32. Kenny, Michael, Presentation at the Fuel Cell Vehicle Technology Conference, UC Davis, Davis, CA, 1998.

33. Kreuer, K.D., "On the complexity of Proton Conduction Phenomena", Solid State Ionics, 136-137, pp 149-160, 2000.

34. Mosdale, R. and Srinivasan, S., "Analysis and Performance and of Water and Thermal Management in Proton Exchange Membrane Fuel Cells", Electrochimica Acta, Vol. 40, No.4, pp. 413-421, 1995.

35. Nguyen, T., and White, R, "A Water and Heat Management Model for PEM fuel Cells", Journal of the Electrochemical Society, Vol. 140, No. 8, pp 2178-2186, 1993.

36. Panik, Ferdinand, "Fuel Cells for Vehicle Applications in Cars – bringing the future closer", Journal of Power Sources, Vol. 71, pp 36-38, 1998.

37. Prater, Keith, "Polymer Electrolyte Fuel Cells: A Review of Recent Developments", Journal of Power Sources, Vol. 51, pp 129-144, 1994.

38. Ramaswamy, S., Sundaresan, M., Eggert, A., Moore, R.M., "System Dynamics and Efficiency of the Fuel Processor for an Indirect Methanol Fuel Cell Vehicle", Proc. of the 35th Intersociety Energy Conversion Engineering Conference, American Institute of Aeronautics and Astronautics, Vol. 2, pp.1372-1377, 2000.

39. Ren, X and Gottesfeld, S., "Electro-Osmotic Drag of Water in Poly (perfluorosulfonic acid) Membranes", Journal of the Electrochemical Society, Vol. 148, No. 1, pp A87-A93, 2001.

40. Sadler, M., Stapleton, A.J., Heath, R.P.G. and Jackson, N.H., "Application of Modeling Techniques to the Design and Development of Fuel Cell Vehicle Systems", Fuel Cell Power for Transportation 2001, Proc. of the SAE 2001 World Congress, pp. 81-90, 2001.

41. Springer, T., Zawodzinski, T., and Gottesfeld, S., "Polymer Electrolyte Fuel Cell Model", Journal of the Electrochemical Society, Vol. 138, No. 8, pp. 2334-2342, 1991.

42. Springer, T. E., M. S. Wilson, S. Gottesfeld, "Modeling and Experimental Diagnostics in Polymer Electrolyte Fuel Cells", Journal of the Electrochemical Society, Vol. 140, pp 3513-3526, 1993.

43. Springer, T. E., T.A. Zawodzinski, M. S. Wilson, S. Gottesfeld, "Characterization of Polymer Electrolyte Fuel Cells Using AC Impedance Spectroscopy", Journal of the Electrochemical Society, Vol. 143, pp 587-599, 1996.

44. Thampan, T., Malhotra, S., Tang, H, and Dutta, R., "Modeling of Conductive Transport in Proton Exchange Membrane Fuel Cells", Journal of the Electrochemical Society, Vol. 147, No. 9., pp 3242-3250, 2000.

45. Um, S., Wang, C.Y., Chen, K.S., "Computational Fluid Dynamics Model of PEM Fuel Cells", Journal of the Electrochemical Society, Vol. 147, No. 12, pp 4485-4493, 2000.

46. Wang, C.Y., and Gu, W.B., "Micro-Macroscopic Modeling of Batteries and Fuel Cells", Journal of the Electrochemical Society, Vol. 145, No. 10, pp 3407-3415, 1998.

47. Wang, Z.H., Wang, C.Y., and Chen, K.S., "Two Phase Flow and Transport in the Air Cathode of PEM Fuel Cells", Journal of Power Sources, Vol. 94, pp 40-50, 2001.

48. Wood, D., Yi, J.S., Nguyen, T.V., "Effect of Direct Liquid Water Injection and Interdigitated Flow Field On the Performance of Proton Exchange Membrane Fuel Cells", Electrochimica Acta, Vol. 43, No. 24, pp 3795-3809, 1998.

49. Yi, J., and Nguyen, T., "An Along-the-Channel Model for Proton Exchange Membrane Fuel Cells", Journal of the Electrochemical Society, Vol. 145, No. 4, 1149-1159, 1998.

Nomenclature

Alpha: Moles of water dragged per mole of hydrogen utilized (no units)

Ac: Heat transfer area of the condenser (m^2)

As: Heat transfer area of the radiator (m^2)

Hfg: Latent heat of vaporization of water (J/mole)

HRR: Heat rejection requirement (kW/C)

m_dot_H2Ostack: Total amount of water condensed inside the stack at any instant (moles/sec)

n_cell: Total number of cells in the stack

nH2O_drag: Total moles of water dragged per cell (moles/sec)

nH2O_drag_tot: Total amount of water dragged in the stack (moles /sec)

nH2_utilized: Moles of hydrogen utilized per cell (moles/sec)

$P_{humidification}$: Power required for humidification (watts)

PEM: proton exchange membrane

P_{stack_gross} : The power output from the terminals of the

fuel cell stack. (watts)

P_{air_system}: The power drawn from the fuel cell stack by the air supply sub-system. (watts)

$P_{condenser}$: The power drawn from the fuel cell stack by the condenser fan. (watts)

$P_{radiator}$: The power drawn from the fuel cell stack by the radiator water pumps and fan. (watts)

P_{aux}: Total power drawn from the fuel cell stack by all auxilaries or sub-systems. (watts)

P_{gross} : Total electric power produced by the stack (watts)

P_{net}: The net power of the fuel cell system – the gross stack power minus any sub-system power draws. (watts)

P_{net_opt}: The maximum net power achievable at a particular current given a specific stack, air supply and WTM sub-system. (watts)

Pr or Pr_{air}: air supply pressure (MPa)

P1: The air supply pressure below which no condensation is done within the stack. (MPa)

P2: The air supply pressure above which no condensation takes place within the condenser. (MPa)

P_opt: The air supply pressure at which the minimum power is drawn from the WTM sub-system. (MPa)

$Q_{radiator\_cond}$:The amount of heat that has to be dissipated by the radiator to account for the water condensed inside the stack (watts)

$Q_{condenser}$: The amount of heat that has to be dissipated by the condenser (watts)

Q_{stack_ineff} : The amount of heat that has to be dissipated by the radiator to account for the stack inefficiency (watts)

Q_{rad_tot} : Total amount of heat that has to be dissipated by the radiator (watts)

SR: Air-side stoichiometric ratio (no units)

SR1: The air supply stoichiometric ratio below which no condensation is takes place within the condenser.

SR2: The air supply stoichiometric ratio above which no condensation is done within the stack.

SR_opt: The air supply pressure at which the minimum power is drawn from the WTM sub-system.

T_{stack} : Stack Temperature (centigrade)

T_{sat} : Temperature at the exit of the condenser at which the required amount of water is condensed (Centigrade)

T_{amb} : Ambient temperature (centigrade)

Us: Heat transfer coefficient (required for condensation) of the radiator (Watts/m^2/K)

Uc: Heat transfer coefficient at the condenser (Watts/m^2/K)

WTM: water and thermal management

Appendix

A1: Cell Model for Anode –Centric Analysis

The intention of this section is to give a conceptual description of the cell model used for the anode-centric analysis by illustrating the major equations used. The model is much more detailed than what will be described in this section. For a more detailed description, the reader is encouraged to read Springer et al. (1991).

Stefan-Maxwell equations are used to model the transport of reactants and water through the gas diffusion-backing layer. A generalized form of the Stefan-Maxwell equation for multi-component diffusion is shown below:

$$\frac{dx_i}{dz} = RT\sum_j \frac{X_i N_j - X_j N_i}{PD_{ij}} \qquad \textbf{Equation 12}$$

Where the subscript "i" is used for the component whose mole fraction is being calculated, and subscript "j" is used for the other components present in the mixture. X is the mole fraction of a given component; N is the molar flux (mol/sq cm./sec.) of the given component; P is the total pressure of the mixture (atm) and D_{ij} is the binary diffusion coefficient (sq cm./sec) between components "i" and "j". For more details on calculation of diffusion coefficients, the reader is encouraged to read Bird et al. (1960).

The electro-osmotic drag is modeled as a function of the membrane water content.

$$n_{drag} = 2.5\lambda / 22 \qquad \textbf{Equation 13}$$

$$N_{w,drag} = 2In_{drag}$$ **Equation 14**

Where n_{drag} is the water drag coefficient i.e the number of molecules of water dragged per proton (H_2O/H^+), λ is the water content of the membrane (H_2O/SO_3^-), $N_{w,drag}$ is the flux of water dragged (mol/sq cm./sec) and I is the hydrogen molar flux (mol/sq cm./sec). The water drag coefficient, n_{drag}, in the above expression is shown to have a linear dependant on the water content of the membrane. Nevertheless, there are other theories on the dependencies of electro-osmotic drag on membrane water content. For example, Ren and Gottesfeld (2001) indicate that for low water contents (λ = 1 to 14), the water drag coefficient is unity. For higher water contents (λ = 14 to 22), the water drag coefficient increases to between 2 and 3 H_2O/H^+. However, in this analysis, the linear dependence of water drag coefficient on membrane water content is employed.

The membrane water content is modeled as a function of water vapor activity till saturation.

$$\lambda = 0.043 + 17.81a - 39.85a^2 + 36a^3 \quad for 0 < a <= 1$$ **Equation 15**

Where "a" is the activity of water.

Above saturation, a linear increase of λ from 14 to 16.8 is allowed

$$1 <= \frac{X_w P}{P_{sat}} <= 3, \quad \lambda = 14 + 1.4(\frac{X_w P}{P_{sat}} - 1)$$ **Equation 16**

Where X_w is the mole fraction of water, P is the pressure (atm), and P_{sat} is the saturation pressure (atm) at 80 C.

The variation of λ across the membrane is calculated by the following equation:

$$\frac{d\lambda}{dz} = [2.2.5.\frac{\lambda}{22} - \alpha]\frac{I.M_m}{D_\lambda(\lambda).\rho_{dry}}$$ **Equation 17**

Where α is the moles of water dragged per mole of hydrogen transported, ρ_{dry} is the density of the membrane (g/cm^3), $D_\lambda(\lambda)$ is the diffusion coefficient of water in the membrane (sq cm./sec) (experimentally measured) and M_m is the equivalent weight of the membrane.

The cathode overpotential loss is calculated using a simple Tafel expression

$$J = j_0 P_c \frac{X_{o\_cat}}{1 - x_{liq}} \exp(\frac{0.5F\eta}{RT})$$ **Equation 18**

Where J is the current density (A/sq cm.), j_0 is the exchange current density (A/sq cm.), X_{o_cat} is the mole fraction of oxygen at the cathode catalyst layer, x_{liq} is the mole fraction of liquid water at the catalyst layer, T is the cell temperature (K), R is the molar gas constant, P_c is the cathode pressure (atm) and η is the overpotential loss (volts). It is understood that the above expression is a simple representation of the cathode overpotential losses. It assumes an infinitely thin catalyst layer and does not take into account the transport losses inside the catalyst layer.

The final voltage is calculated using the following equation

$$V_{cell} = V_{oc} - \eta - J.R_{mem}$$ **Equation 19**

Where V_{cell} is the cell voltage (volts), V_{oc} is the open circuit voltage (volts), η is the cathode overpotential loss (volts), and R_{mem} is the membrane resistance (ohms sq cm.). Anode overpotential losses are assumed to be zero.

A2: Cell Model for Cathode-Centric Analysis

This section briefly describes the cell model used for the cathode-centric analysis. The cell model for the cathode-centric analysis is different from the one used for the anode-centric analysis. As the objective is to capture all the cathode losses, the cathode is modeled in detail. Apart from modeling the transport processes in the gas diffusion layer, the transport processes in the catalyst layer are also modeled. Unlike the model used for the anode-centric analysis, this model assumes a constant membrane resistance. For details on modeling, the reader is encouraged to read Springer et al. (1993) and Springer et al. (1996).

The following losses are taken into account in the model.

- Cathode losses
    - Reaction losses due to the reduction of oxygen at the cathode
    - Protonic resistance losses in the catalyst layer
    - Oxygen permeability losses in the catalyst layer
    - Transport losses in the cathode gas diffusion backing layer
- Ionic membrane resistance losses

Anode overpotential losses are assumed to be zero. Equation 20 illustrates the final cell voltage calculation equation.

$$V_{cell} = \left(V_{ref} - R_{cell} \cdot I - \eta_{cathode}(p_{ox}, I)\right)$$

where:

V_{cell} = Cell voltage [V]

V_{ref} = Reference cell voltage [V]

I = Cell current [A]

R_{cell} = Cell resistance [Ω]

$\eta_{cathode}$ = Cathode overpotential [V]

p_{ox} = Partial pressure of oxygen at the cathode catalyst layer[Pa]

Equation 20

It can be noticed that the cathode overpotential losses are a function of the current and the partial pressure of oxygen at the cathode catalyst layer.